Tsallis fits to p_T spectra and multiple hard scattering in pp collisions at the LHC

Cheuk-Yin Wong

Oak Ridge National Laboratory, Physics Division, Oak Ridge, Tennessee 37831, USA

Grzegorz Wilk

National Centre for Nuclear Research, Warsaw 00-681, Poland

Phenomenological Tsallis fits to the CMS, ATLAS, and ALICE transverse momentum spectra of hadrons for pp collisions at LHC were recently found to extend over a large range of the transverse momentum. We investigate whether the few degrees of freedom in the Tsallis parametrization may arise from the relativistic parton-parton hard-scattering and related processes. The effects of the multiple hard-scattering and parton showering processes on the power law are discussed. We find empirically that whereas the transverse spectra of both hadrons and jets exhibit power-law behavior of $1/p_T^n$ at high p_T, the power indices n for hadrons are systematically greater than those for jets, for which $n \sim 4$–5.

I. INTRODUCTION

The transverse momentum distributions of produced particles in hadron and nuclear collisions provide useful information on the dynamics of the colliding system. The low-p_T part of the spectra falls within the realm of soft nonperturbative QCD physics and may involve the parton wave functions in a flux tube [1], the thermodynamics[1] and the recombination of partons [2–13], or the fragmentation of a QCD string [14]. On the other hand, the high-p_T part is usually considered to arise from a perturbative QCD hard scattering between a parton of one hadron and a parton of the other hadron [15–22]. The borderline between the soft-p_T nonperturbative region and the high-p_T perturbative region is not well determined. A very different scheme to partition the p_T spectrum into soft and hard components has also been suggested [23,24] and will be discussed at the end of this paper.

In recent RHIC and LHC experiments, the transverse momentum spectra of charged hadrons for pp and nucleus-nucleus collisions have been measured at very high energies [25–30]. These spectra are often described by the Tsallis distribution [6],

---

*wongc@ornl.gov

†wilk@fuw.edu.pl

[1]The usual (extensive) thermodynamics with the Boltzmann-Gibbs distribution have been described in [2–4] and applied extensively for multiparticle production in [5]. Its nonextensive generalization with the Tsallis distribution with a new nonextensivity parameter q has been given in [6]. The nonextensive statistical approach has been very successful in describing many different physical systems, including multiparticle production processes at lower energies. See Refs. [7–13] for a summary of earlier attempts to use Tsallis fits and detailed explanations of the possible meaning of the q parameter.

$$h_q(p_T) = C_q \left[1 - (1-q) \frac{p_T}{T} \right]^{\frac{1}{1-q}}, \qquad (1)$$

with a normalization constant C_q, a "temperature" T, and a dimensionless nonextensivity parameter q (with $q > 1$). The Tsallis distribution can be regarded as a nonextensive generalization of the usual exponential (Boltzmann-Gibbs) distribution, and converges to it when the parameter q tends to unity,

$$h(p_T) \xrightarrow{q \to 1} C_1 \exp\left(-\frac{p_T}{T} \right). \qquad (2)$$

It has been very successful in describing very different physical systems in terms of a statistical approach, including multiparticle production processes at lower energies [7–13].

On the other hand, a long time ago Hagedorn proposed the *QCD inspired* empirical formula to describe experimental hadron production data as a function of p_T over a wide range [2]:

$$E \frac{d^3\sigma}{d^3p} = C \left(1 + \frac{p_T}{p_0} \right)^{-n} \to \begin{cases} \exp\left(-\frac{n p_T}{p_0} \right) & \text{for } p_T \to 0, \\ \left(\frac{p_0}{p_T} \right)^n & \text{for } p_T \to \infty, \end{cases} \qquad (3)$$

where C, p_0, and n are fitting parameters. This becomes a purely exponential function for small p_T and a purely power-law function for large p_T values.[2] It coincides with Eq. (1) for

$$n = \frac{1}{q-1} \quad \text{and} \quad p_0 = \frac{T}{q-1}. \qquad (4)$$

Usually both formulas are treated as equivalent from the point of view of phenomenological fits and are often used

---

[2]Actually the QCD formula was inspired by related work in [15–18] and proposed earlier in [31,32].

interchangeably [25–30]. It is worth stressing that both Eqs. (1) and (3) describe data *in the whole region of transverse momenta,* not only for large p_T.

For phenomenological as well as theoretical interests, it is expected that as the low-p_T region and the high-p_T region arise from different mechanisms, there can be a change of the systematics for the description of the low-p_T nonperturbative QCD region and the high-p_T perturbative QCD region. It is therefore useful to explore where the Tsallis fit begins to fail at higher and higher p_T in the recent high-p_T data of CMS [27,28], ATLAS [29], and ALICE Collaborations [30] for pp collisions at the LHC. An excellent fit to the p_T hadron spectra was earlier obtained there with the Tsallis and/or Hagedorn distributions for p_T from 0.5 GeV up to 6 GeV, in pp collisions at $\sqrt{s} = 7$ TeV [27]. It was however a surprise to find that the phenomenological Tsallis fits to the CMS and ATLAS charged particle transverse spectra extends from $p_T = 0.5$ to 181 GeV/c in pp collisions at $\sqrt{s} = 7$ TeV, and from $p_T = 0.5$ to 31 GeV/c at $\sqrt{s} = 0.9$ TeV [33]. The simplicity of the Tsallis parametrization with only three parameters and the large range of the fitting transverse momentum raise questions on the physical meaning of the degrees of freedom that enter into the high-p_T distribution.

As the magnitude of the transverse momenta in these high-p_T data are much greater than the mean transverse momentum of the distribution, concepts such as statistical mechanics that depend on thermodynamical equilibrium or quasiequilibrium may be subject to question. The asymmetry between the transverse and the longitudinal degrees of freedom also poses additional difficulties in a statistical explanation of the full three-dimensional momentum distribution.[3]

To describe the transverse momentum distribution in the high p_T region, a more natural description would be to employ the relativistic hard-scattering model in perturbative QCD. We wish to investigate whether the few degrees of freedom in the transverse momentum Tsallis distribution may arise from the basic parton-parton scattering and the accompanying multiple collision and showering processes.

The relativistic hard-scattering model has been used previously to examine inclusive particle production in hadron-hadron collisions [15–22]. It was found earlier on that the observed experimental hadron transverse differential cross section appears to differ from what one expects from naive point parton collisions. In the basic quark model, the high-p_T differential cross section in an $ab \rightarrow cd$ exclusive process can be inferred from the counting rule of Brodsky, Farrar, Matveev *et al.* [36,37], which

states that the invariant cross section for the exclusive process at high-p_T behaves as the power law, with power index n,

$$E_c \frac{d\sigma(ab \rightarrow cd)}{dc^3} \propto \frac{1}{c_T^n}, \qquad (5)$$

where $n = 2 \times \{(\text{number of active participants}) - 2\}$. The counting of the number of active participants includes constituents in the initial ab and the final cd states. (For a pedagogical discussion of the counting rule, see [19].) The counting rule of Brodsky, Farrar, Matveev *et al.* [36,37] has been found to give a power index n that agrees reasonably with experimental data for exclusive $ab \rightarrow cd$ processes [38]. If one assumes that the dominant basic high-p_T parton-parton hard-scattering process in a pp collision comes from $qq \rightarrow qq$ (or other $2 \rightarrow 2$ processes), then the counting rule gives a transverse momentum dependence of $d\sigma/dt \sim 1/p_T^n$ with $n = 4$. However, the observed experimental power index n of the hadron transverse spectrum is about 7 (even at the highest LHC energy and for very large transverse momenta measured [33]). If one assumes that the basic process is $q + \text{meson} \rightarrow q + \text{meson}$, then the counting rule gives $n = 8$ which is close to the observed value. Blankenbecler, Brodsky, and Gunion therefore proposed that the power index of $n \sim 8$ may be related to the scattering of a parton with a meson [16–18]. For pp collisions at the LHC, a modified proposal with the direct meson production in the basic reaction $g + q \rightarrow \text{meson} + q$ has been suggested recently, involving five active participants and $n = 6$ for the power index [21,22].

We will however not work with mesons as elementary participant constituents as in [16–18,21,22] but will work within the conventional parton model of quarks and gluons. The collision of hadrons (or nuclei) consists of the collisions of partons either in parallel or in series. For example, in the PYTHIA Monte Carlo program, the multiple hard scattering of partons in parallel is an important ingredient and the number of hard-scattering interactions per inelastic event may be greater than unity [20]. The other process of multiple scattering of partons in series has been examined in great detail previously [39–48]. Remarkably, a simple picture emerges from these studies to indicate that as a result of the multiple scattering, the sum of the multiple collision series in a minimum-biased sampling at high p_T is dominated by the differential cross section for the single parton-parton scattering. As a result of shadowing cancellations, the high-p_T scattering appears as though it arises from a single scattering with a $1/p_T^4$ distribution, plus logarithmic residue terms. This remarkable result was shown in [46], using an auxiliary generating functional. We would like to follow and extend the multiple hard-scattering results of [46], in order to obtain an explicit form of the multiple scattering power law and logarithmic residue terms, the dependence on the number of partons,

---

[3]However, it should be remembered that the statistical approach is not the only known source of Tsallis distribution in Eq. (1). There are numerous dynamical mechanisms leading to it, see [8,34,35].

the dependence on the number of scatterers, and the dependence on the centrality of the collision. These new results may find applications in the multiple hard-scattering processes in hadron-hadron as well as nucleus-nucleus collisions.

Whereas the theoretical analyses of [39–48] indicate that the multiple scattering process involving partons will not significantly modify the $1/p_T^4$ distribution of the high-p_T transverse differential cross section with $n = 4$, the PYTHIA program with properly tuned sets of parameters in a relativistic hard-scattering model, with the additional processes of parton showering and radiations, can describe quite well the transverse momentum distribution of produced hadrons in pp collisions at LHC energies [27] with $n \sim 7$ [33]. What is the origin of such a difference in the power indices n? Could the additional process of parton showering and hadronization affect the power index n?

The possibility that parton showering and hadronization may influence the power index n is revealed by the measurements of the transverse differential cross section of hadron and photon jets for $p\bar{p}$ collisions at Fermilab by the CDF and D0 collaborations [49–53]. In these measurements, the power indices n are found to be close to $n = 4$–5 (see Fig. 2 of [21]), as predicted from perturbative QCD. A hadron jet in these measurements corresponds to a collection of hadrons in calorimeter cells contained within a cone of opening angle R, and it represents a parton after a parton-parton collision but before its fragmentation and hadronization. Its transverse momentum differential cross section retains the main features of the power law of $1/p_T^4$ of the basic parton-parton hard scattering. Thus, the difference between the power index of $n \sim 4$–5 from the jet transverse differential cross section and $n \sim 7$ from the hadron spectra is likely related to the subsequent showering and hadronization of the parton jets to hadron fragments of lower transverse momenta. We would like to examine here how the additional process of parton fragmentation and parton showering may influence the power index of the transverse differential cross section.

This paper is organized as follows. In Sec. II, we review the relativistic hard-scattering model to express the scattering cross section for high-p_T processes in terms of the basic parton-parton differential cross sections. An approximate analytical expression is obtained by carrying out the hard-scattering integral analytically. In Sec. III, we study the effects of multiple hard scattering of partons on the differential cross sections. In Sec. IV, we include the effects of the additional dependence of the parton thickness function $T(b)$ on the parton differential cross sections. In Sec. V, we analyze the experimental results of jet transverse differential cross sections with the relativistic hard-scattering model and find the approximate validity of the relativistic hard-scattering (rhs) model for jet production. In Sec. VI, we examine the effect of fragmentation on the hadron differential cross section. In Sec. VII, we study the effects of showering and its effects on the power index. In Sec. VIII, we fit the experimental CMS, ATLAS, and ALICE data to the hard-scattering model and extract the power index from data. In Sec. IX, we present our discussions and conclusions.

II. RELATIVISTIC HARD SCATTERING MODEL

We review some of the earlier results in the relativistic hard scattering model [15–19,54]. We consider the process of $A + B \to c + X$ with the production of parton c around $\eta \sim 0$ in the center-of-mass frame of the A-B system. We shall later consider the fragmentation of the parton c in Sec. V and the showering process in Sec. VI. The differential cross section for this process is given in the parton model by

$$E_c \frac{d^3\sigma(AB \to cX)}{dc^3} = \sum_{ab} \int dx_a d\boldsymbol{a}_T dx_b d\boldsymbol{b}_T G_{a/A}(x_a, \boldsymbol{a}_T) G_{b/B}(x_b, \boldsymbol{b}_T) E_c \frac{d^3\sigma(ab \to cX')}{dc^3}. \tag{6}$$

We consider the basic process to be the lowest-order elastic parton-parton collisions in which the parton-parton invariant cross section is related to $d\sigma/dt$ by

$$E_c \frac{d^3\sigma(ab \to cX')}{dc^3} = \frac{\hat{s}}{\pi} \frac{d\sigma(ab \to cX')}{dt} \delta(\hat{s} + \hat{t} + \hat{u}), \tag{7}$$

where we have neglected the rest masses and we have introduced

$$\hat{s} = (a + b)^2, \qquad \hat{t} = (a - b)^2, \qquad \hat{u} = (b - c)^2.$$

We write out the momenta in the infinite momentum frame, with $\sqrt{s}$ the center-of-mass energy of the A-B system,

$$a = \left(x_a \frac{\sqrt{s}}{2} + \frac{a_T^2}{2x_a\sqrt{s}}, \boldsymbol{a}_T, x_a \frac{\sqrt{s}}{2} - \frac{a_T^2}{2x_a\sqrt{s}}\right),$$

$$b = \left(x_b \frac{\sqrt{s}}{2} + \frac{b_T^2}{2x_b\sqrt{s}}, \boldsymbol{b}_T, -x_b \frac{\sqrt{s}}{2} + \frac{b_T^2}{2x_b\sqrt{s}}\right),$$

$$c = \left(x_c \frac{\sqrt{s}}{2} + \frac{c_T^2}{2x_c\sqrt{s}}, \boldsymbol{c}_T, x_c \frac{\sqrt{s}}{2} - \frac{c_T^2}{2x_c\sqrt{s}}\right).$$

The light-cone variable x_c of the produced parton c is

$$x_c = \frac{c_0 + c_z}{\sqrt{s}}. \tag{8}$$

The Mandelstam variables are

$$\hat{s} = (a + b)^2 = x_a x_b s + \frac{a_T^2 b_T^2}{x_a x_b s} - 2\boldsymbol{a}_T \cdot \boldsymbol{b}_T,$$

$$\hat{t} = (a - c)^2 = -\frac{x_a c_T^2}{x_c} - \frac{x_c a_T^2}{x_a} + 2\boldsymbol{a}_T \cdot \boldsymbol{c}_T,$$

$$\hat{u} = (b - c)^2 = -x_b x_c s - \frac{b_T^2 c_T^2}{x_b x_c s} + 2\boldsymbol{b}_T \cdot \boldsymbol{c}_T.$$

The relation of $\hat{s} + \hat{t} + \hat{u} = 0$ gives

$$x_a x_b s + \frac{a_T^2 b_T^2}{x_a x_b s} - \frac{x_a c_T^2}{x_c} - \frac{x_c a_T^2}{x_a} - x_b x_c s - \frac{b_T^2 c_T^2}{x_b x_c s}$$
$$= -a_T^2 - b_T^2 - c_T^2 + (\boldsymbol{c}_T - \boldsymbol{a}_T + \boldsymbol{b}_T)^2. \quad (9)$$

Because the intrinsic a_T and b_T are small compared with the magnitudes of a_z, b_z, and c_T, we can therefore neglect terms with a_T and b_T in the evaluation of $\hat{s}$, $\hat{t}$, and $\hat{u}$. We get

$$\hat{s} = x_a x_b s, \qquad \hat{t} = -\frac{x_a c_T^2}{x_c}, \qquad \hat{u} = -x_b x_c s. \quad (10)$$

The constraint of $\hat{s} + \hat{t} + \hat{u} = 0$ gives

$$x_a(x_b) = x_c + \frac{c_T^2}{(x_b - \frac{c_T^2}{x_c s})s}. \quad (11)$$

In the special case of particle c coming out at $\theta_c = 90°$ in the center-of-mass frame of the A-B system,

$$x_c = \frac{c_T}{\sqrt{s}}, \qquad x_a(x_b) = x_c + \frac{x_c^2}{x_b - x_c}, \quad (12)$$

and

$$x_a = x_b = 2x_c. \quad (13)$$

The constraint in Eq. (7) can be written as a constraint in x_a,

$$\delta(\hat{s} + \hat{t} + \hat{u}) = \frac{\delta(x_a - x_a(x_b))}{|\frac{\partial(\hat{s} + \hat{t} + \hat{u})}{\partial x_a}|}. \quad (14)$$

On the other hand,

$$\frac{\partial(\hat{s} + \hat{t} + \hat{u})}{\partial x_a} = s\left(x_b - \frac{c_T^2}{x_c s}\right). \quad (15)$$

We have therefore

$$E_c \frac{d^3\sigma(ab \to cX')}{dc^3} = \frac{d\sigma(ab \to cX)}{dt} \frac{x_a x_b \delta(x_a - x_a(x_b))}{\pi(x_b - c_T^2/x_c s)}, \quad (16)$$

and

$$E_c \frac{d^3\sigma(AB \to cX)}{dc^3}$$
$$= \sum_{ab} \int d\boldsymbol{a}_T d\boldsymbol{b}_T dx_b dx_a$$
$$\times G_{a/A}(x_a, \boldsymbol{a}_T) G_{b/B}(x_b, \boldsymbol{b}_T)$$
$$\times \frac{x_a x_b \delta(x_a - x_a(x_b))}{\pi(x_b - c_T^2/x_c s)} \frac{d\sigma(ab \to cX')}{dt}. \quad (17)$$

We consider an approximate structure function of the form

$$G_{a/A}(x_a, \boldsymbol{a}_T) = \frac{A_a}{x_a}(1 - x_a)^{g_a} D_a(\boldsymbol{a}_T),$$

$$G_{b/B}(x_b, \boldsymbol{b}_T) = \frac{A_b}{x_b}(1 - x_b)^{g_b} D_b(\boldsymbol{b}_T).$$

The integral in Eq. (17) becomes

$$E_c \frac{d^3\sigma(AB \to cX)}{dc^3}$$
$$= \sum_{ab} A_a A_b \int d\boldsymbol{a}_T d\boldsymbol{b}_T D_a(\boldsymbol{a}_T) D_b(\boldsymbol{b}_T)$$
$$\times dx_b dx_a (1 - x_a)^{g_a} (1 - x_b)^{g_b}$$
$$\times \frac{\delta(x_a - x_a(x_b))}{\pi(x_b - c_T^2/x_c s)} \frac{d\sigma(ab \to cX')}{dt}.$$

We integrate over x_a, and we get

$$E_C \frac{d^3\sigma(AB \to cX)}{dc^3} = \sum_{ab} A_a A_b \int d\boldsymbol{a}_T d\boldsymbol{b}_T D_a(\boldsymbol{a}_T) D_b(\boldsymbol{b}_T)$$
$$\times dx_b \frac{(1 - x_a)^{g_a} (1 - x_b)^{g_b}}{\pi(x_b - c_T^2/x_c s)}$$
$$\times \frac{d\sigma(ab \to cX')}{dt}.$$

As the transverse momentum we are considering is considerably larger than the intrinsic p_T [54], we can take the intrinsic momentum distribution to be quite narrow so that the integration of $\int d\boldsymbol{a} D_a(\boldsymbol{a}_T) = \int d\boldsymbol{b} D_b(\boldsymbol{b}_T) = 1$ and we obtain

$$E_C \frac{d^3\sigma(AB \to cX)}{dc^3} = \sum_{ab} A_a A_b \int dx_b \frac{(1 - x_a)^{g_a} (1 - x_b)^{g_b}}{\pi(x_b - \tau_c^2)}$$
$$\times \frac{d\sigma(ab \to cX')}{dt}, \quad (18)$$

where we have introduced

$$\tau_c^2 = \frac{c_T^2}{s}. \quad (19)$$

We use the saddle point integration method [54] and get

$$E_C \frac{d^3\sigma(AB \to cX)}{dc^3} = \sum_{ab} A_a A_b \int dx_b \frac{e^{f(x_b)}}{\pi(x_b - \tau_c^2/x_c)}$$
$$\times \frac{d\sigma(ab \to cX')}{dt}, \qquad (20)$$

with

$$f(x_b) = g_a \ln(1 - x_a) + g_b \ln(1 - x_b).$$

Consider $g_a = g_b = g$ and expand $f(x_b)$ as a function of x_b about the minimum located at

$$x_{b0} = \frac{\tau_c^2}{x_c} + \tau_c \sqrt{\frac{1 - \tau_c^2/x_c}{1 - x_c}}. \qquad (21)$$

The quantity x_a at this minimum is

$$x_{a0} = x_c + \tau_c \sqrt{\frac{1 - x_c}{1 - \tau_c^2/x_c}}. \qquad (22)$$

From the second derivative of $f(x_b)$ with respect to x_b, we obtain

$$E_c \frac{d^3\sigma(AB \to cX)}{dc^3}$$
$$\sim \sum_{ab} \frac{A_a A_b}{\sqrt{\pi g_a}} (1 - x_{a0})^{g_a} (1 - x_{b0})^{g_a} \frac{1}{\sqrt{\tau_c}} \left\{ \frac{1 - x_c}{1 - \tau_c^2/x_c} \right\}^{1/4}$$
$$\times \sqrt{\frac{(1 - x_{b0})^2}{[1 - (x_{b0} + \tau_c^2/x_c)/2]}} \frac{d\sigma(ab \to cX')}{dt} \Bigg|_{x_{a0}, x_{b0}}. \qquad (23)$$

In the neighborhood of $\theta_c \sim 90°$ in the A-B center-of-mass system, the ratios in the square-root factor and the factor involving the power $1/4$ are approximately equal to 1. Thus, the analytical integration of the hard-scattering integral leads to the following invariant differential cross section in an analytical form,

$$E_c \frac{d^3\sigma(AB \to cX)}{dc^3} \sim \sum_{ab} \frac{A_a A_b}{\sqrt{\pi g_a}} (1 - x_{a0})^{g_a} (1 - x_{b0})^{g_a}$$
$$\times \frac{1}{\sqrt{\tau_c}} \frac{d\sigma(c_T; ab \to cX')}{dt} \Bigg|_{x_{a0}, x_{b0}}. \qquad (24)$$

As an example, we can consider the basic $ab \to cX'$ process to be $gg \to gg$. The cross section as given by Gastman and Wu [55] (page 403) is

$$\frac{d\sigma(gg \to gg)}{dt} = \frac{9\pi\alpha_s^2}{8} \frac{(\hat{s}^4 + \hat{t}^4 + \hat{u}^4)((\hat{s}^2 + \hat{t}^2 + \hat{u}^2)}{\hat{s}^4 \hat{t}^2 \hat{u}^2}.$$

At $\theta \sim 90°$, we have

$$\frac{d\sigma(gg \to gg)}{dt} = \frac{9\pi\alpha_s^2}{16c_T^4} \left[1 + \left(\frac{c_T^2}{x_c x_b s} \right)^2 + \left(\frac{x_c}{x_a} \right)^2 \right]^3$$
$$\sim \frac{9\pi\alpha_s^2}{16c_T^4} \left[\frac{3}{2} \right]^3. \qquad (25)$$

If one considers the $qq' \to qq'$ process, then

$$\frac{d\sigma(qq' \to qq')}{dt} = \frac{4\pi\alpha_s^2}{9} \frac{\hat{s}^2 + \hat{u}^2}{\hat{s}^2 \hat{t}^2}. \qquad (26)$$

At $\theta_c \sim 90°$, we have $x_a = 2x_c$, and we have for $qq' \to qq'$

$$\frac{d\sigma(qq' \to qq')}{dt} = \frac{4\pi\alpha_s^2}{9c_T^4} \frac{5}{16}. \qquad (27)$$

In either case, the differential cross section varies as $d\sigma(ab \to cX')/dt \sim \alpha_s^2/c_T^4$.

III. EFFECTS OF MULTIPLE SCATTERING OF PARTONS ON DIFFERENTIAL CROSS SECTIONS

Hadrons are composite objects containing a number of partons. The collision of hadrons involves the soft and hard collisions of partons. We separate the total parton-parton cross section σ_{in} into soft and hard parts, $\sigma_{in}(\text{parton-parton}) = \sigma_s + \sigma_H$, where σ_s involves soft processes at low-p_T in the fragmentation of partons in a flux tube or a string. The hard cross section σ_H involves infrared singularities at small momentum transfer which can be regulated by a minimum momentum transfer cutoff p_0 that delimits the boundary between soft and hard processes. The parton-parton hard cross section includes the cross section for the production of high-p_T particles and mini-jets.

With increasing collision energies, we probe regions of smaller x, where the parton density increases rapidly. The number of partons and the total hard-scattering cross section in pp collisions increases with increasing collision energies. The total pp hard-scattering cross section may exceed the inelastic pp total cross section at high energies [20]. The average number of parton-parton interactions above a minimum p_0 may be greater than unity.

The presence of a large number of partons in the colliding system leads to parton multiple scattering in which a projectile parton may make multiple hard scattering with target partons (also called the rescattering of partons). Furthermore, in a hadron-nucleus collision, there are partons in nucleons along the incident parton trajectory, and multiple hard scattering of the incident parton with many target partons may occur.

We consider the scattering from an incident parton a to the final parton c after colliding with two hard scatterers b_1, and b_2 in the process

$$a + (b_1 + b_2) \to c + (d_1 + d_2), \qquad (28)$$

as represented by the Feynman diagram in Fig. 1. For simplicity, we neglect intrinsic p_T and rest masses so that
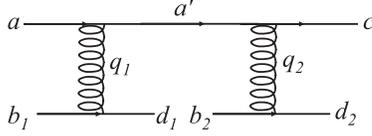
FIG. 1.   The Feynman diagram for the multiple hard scattering process, $a + (b_1 + b_2) \rightarrow c + (d_1 + d_2)$, with the exchange of gluons q_1 and q_2.
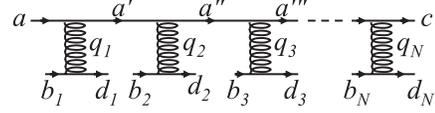

FIG. 2.   The Feynman diagram for the hard scatterings process $a + (b_1 + b_2 + \cdots + b_N) \rightarrow c + (d_1 + d_2 + \cdots + d_N)$, with the exchange of N gluons $q_1, q_2, \ldots, q_N$.

$\boldsymbol{a}_T = \boldsymbol{b}_{T1} = \boldsymbol{b}_{T2} = 0$. We are interested in hard-scattering processes and consider the collision to take place in the center-of-mass system of a and the partons $(b_1 + b_2)$ so that the incident a comes along the longitudinal z axis and comes out as the final particle c in the transverse direction at $\theta_c \sim 90°$. We shall examine here the influence of the multiple hard-scattering process on the differential cross section from parton a to parton c.

The scattering between a and b_i in Fig. 1, with $i = 1, 2$, is individually a hard scattering process with the transfer of a substantial amount of the transverse momentum $\boldsymbol{q}_{Ti}(= \boldsymbol{d}_{Ti})$. The transverse coherence time $\hbar/(|\boldsymbol{q}_{Ti}|c)$, which is also the hard-scattering transverse collision time, is quite short (of the order of 0.01–0.1 fm/c). On the other hand, at high energies the total hard-scattering cross section is of the order of the pp inelastic cross section. The mean-free path λ between parton hard-scattering collisions is of the order of the transverse radius of the proton. Therefore, in a multiple hard-scattering process, the mean-free time λ/c between hard-scattering collisions is much greater than the transverse hard-collision time $\hbar/(|\boldsymbol{q}_{Ti}|c)$.

As a consequence, the sequence of hard-scattering collisions of the incident parton a with scatterers b_1 and b_2 are incoherent collisions. The hard-scattering process $a + b_1 \rightarrow a' + d_1$ has been completed before the other hard-scattering process $a' + b_2 \rightarrow c + d_2$ begins. This implies that the hard-scattering process $a + b_1 \rightarrow a' + d_1$ and the other hard-scattering process $a' + b_2 \rightarrow c + d_2$ in Fig. 1 are separately successive two-body hard-scattering processes with the intermediate particle a' essentially on the mass shell. These successive hard scatterings can be represented by scattering laws $d\sigma(ab_1 \rightarrow a'd_1)/d\boldsymbol{q}_{Ti} \propto \alpha_s^2/(\boldsymbol{q}_{Ti}^2)^2$ and $d\sigma(a'b_2 \rightarrow cd_2)/d\boldsymbol{q}_{T2} \propto \alpha_s^2/(\boldsymbol{q}_{T2}^2)^2$, with the differential elements $d\boldsymbol{d}_{Ti} = d\boldsymbol{q}_{Ti}$. The differential cross section after the multiple hard-scattering collisions with partons in the other hadron is therefore

$$d\sigma_H^{(2)}(a + (b_1 + b_2) \rightarrow c + (d_1 + d_2))$$

$$\propto \frac{d\boldsymbol{c}_T \alpha_s^2 d\boldsymbol{q}_{T1} \alpha_s^2 d\boldsymbol{q}_{T2}}{(\boldsymbol{q}_{T1}^2)^2 (\boldsymbol{q}_{T2}^2)^2} \delta(\boldsymbol{c}_T + \boldsymbol{q}_{T1} + \boldsymbol{q}_{T2}), \quad (29)$$

where the factor $\alpha_s^4/[(\boldsymbol{q}_{T1}^2)^2(\boldsymbol{q}_{T2}^2)^2]$ comes from the the two gluon propagators in Fig. 1. The hard-scattering cross section from a to c, $d\sigma_H^{(2)}(a \rightarrow c)$, can be obtained from

the above by integrating over $\boldsymbol{q}_{T1}$ and $\boldsymbol{q}_{T2}$, regulated by a minimum momentum transfer cutoff p_0.

We can generalize the above result for the scattering of the parton a into the parton c after making a multiple hard scattering with N hard scatterers as shown in the Feynman diagram in Fig. 2,

$$a + (b_1 + b_2 + \cdots + b_N) \rightarrow c + (d_1 + d_2 + \cdots + d_N). \tag{30}$$

Using arguments similar to those leading to Eq. (29), the differential cross section for the multiple hard scattering of a to c after colliding with N hard scatterers in the other hadron is

$$d\sigma_H^{(N)}(a + (b_1 + \cdots + b_N)) \rightarrow c + (d_1 + \cdots + d_N))$$

$$\propto d\boldsymbol{c}_T \prod_{i=1}^N \left(\frac{\alpha_s^2 d\boldsymbol{q}_{Ti}}{(\boldsymbol{q}_{Ti}^2)^2} \right) \delta(\boldsymbol{c}_T + \boldsymbol{q}_{T1} + \cdots + \boldsymbol{q}_{TN}), \tag{31}$$

where the factor $\alpha_s^{2N}/[(\boldsymbol{q}_{T1}^2)^2 \cdots (\boldsymbol{q}_{TN}^2)^2]$ comes from the N gluon propagators in Fig. 2. The hard-scattering cross section from a to c, $d\sigma_H^{(N)}(a \rightarrow c)$, can be obtained from the above by integrating over $\boldsymbol{q}_{T1}, \ldots, \boldsymbol{q}_{TN}$, regulated by a minimum momentum transfer cutoff of p_0.

IV. EFFECTS OF THE MULTIPLE SCATTERING AND $T(b)$ ON THE TRANSVERSE DIFFERENTIAL CROSS SECTION

The discussions in the last section pertain to the differential cross section in the scattering of a parton with N parton scatterers. A hadron-hadron collision consists of a weighted sum of parton-parton collision with different number of scatterers N, depending on the transverse profile of the composite target system and the selection of the centrality of the collision events.

From the earlier studies of multiple hard-scattering processes [39–48], a simple picture emerges to indicate that for high p_T in minimum-biased events without centrality selection, the sum of the multiple collision series over different number of scatterers is dominated by the single scattering differential cross section with the $1/p_T^4$ dependency. There are in addition interesting shadowing cancellations to give logarithmic residual terms. We would like to extend the multiple hard-scattering results of [46] to obtain the explicit power law and logarithmic dependence of the multiple scattering cross section on target scatterer number

N, the dependence on target parton number A, as well as on the centrality of the collision.

The parton-parton hard-scattering cross section σ_H will shadow hard scattering of the colliding partons. Thus, for the collision of a parton a on the object b with A partons, the probability for N hard-scattering collisions at an impact parameter b is [56]

$$P(N, \boldsymbol{b}) = \frac{A!}{N!(A-N)!}[T(b)\sigma_H]^N[1-T(b)\sigma_H]^{A-N}. \quad (32)$$

The total hard-scattering cross section for the scattering of a on N partons is

$$\sigma_H^{(\text{tot})}(a + A \rightarrow cX)$$
$$= \int d\boldsymbol{b} \sum_{N=1}^{A} \frac{A!}{N!(A-N)!}[T(b)\sigma_H]^N[1-T(b)\sigma_H]^{A-N}. \quad (33)$$

Thus, the total differential cross section is

$$\frac{d\sigma_H^{(\text{tot})}(a+A \rightarrow cX)}{d\boldsymbol{c}_T} = \int d\boldsymbol{b} AT(b) \frac{d\sigma_H^{(1)}}{d\boldsymbol{c}_T} \left\{ \{1 - (A-1)[T(b)\sigma_H] + \frac{(A-1)(A-2)}{2}[T(b)\sigma_H]^2 \} \right.$$
$$+ \int d\boldsymbol{b} \frac{A(A+1)/}{2}[T(b)]^2 \frac{d\sigma_H^{(2)}}{d\boldsymbol{c}_T}\{1 - (A-2)[T(b)\sigma_H]\}$$
$$+ \int d\boldsymbol{b} \frac{A(A+1)(A+2)}{6}[T(b)]^3 \frac{d\sigma_H^{(3)}}{d\boldsymbol{c}_T} + \cdots. \quad (36)$$

After expanding the absorption term $[1 - T(b)\sigma_H]^{A-N}$, we can collect all terms of the same order in α_s^{2N} to resum Eq. (34) in the form

$$\frac{d\sigma_H^{(\text{tot})}(a + A \rightarrow cX)}{d\boldsymbol{c}_T}$$
$$= \int d\boldsymbol{b} \sum_{n=1}^{N} \frac{A!}{A!(A-N)!}[T(b)]^N \frac{d\tilde{\sigma}_H^{(N)}}{d\boldsymbol{c}_T}, \quad (37)$$

where $d\tilde{\sigma}_H^{(N)}/d\boldsymbol{c}_T$ is of order α_s^{2N} given by

$$\frac{d\tilde{\sigma}_H^{(1)}}{d\boldsymbol{c}_T} = \frac{d\sigma_H^{(1)}}{d\boldsymbol{c}_T}, \quad (38a)$$

$$\frac{d\tilde{\sigma}_H^{(2)}}{d\boldsymbol{c}_T} = \frac{d\sigma_H^{(2)}}{d\boldsymbol{c}_T} - \frac{2(A-1)}{A+1} \frac{d\sigma_H^{(1)}}{d\boldsymbol{c}_T} \sigma_H, \quad (38b)$$

$$\frac{d\tilde{\sigma}_H^{(3)}}{d\boldsymbol{c}_T} = \frac{d\sigma_H^{(3)}}{d\boldsymbol{c}_T} - \frac{3(A-2)}{(A+2)} \frac{d\sigma_H^{(2)}}{d\boldsymbol{c}_T} \sigma_H$$
$$+ \frac{3(A-1)(A-2)}{(A+1)(A+2)} \frac{d\sigma_H^{(1)}}{d\boldsymbol{c}_T} \sigma_H^2. \quad (38c)$$

The last term in Eq. (38b) and the last terms in Eq. (38c) represent shadowing corrections due to the absorption

$$\frac{d\sigma_H^{(\text{tot})}(a + A \rightarrow cX)}{d\boldsymbol{c}_T}$$
$$= \int d\boldsymbol{b} \sum_{N=1}^{A} \frac{A!}{N!(A-N)!}[T(b)]^N \frac{d\sigma_H^{(N)}}{d\boldsymbol{c}_T}[1 - T(b)\sigma_H]^{A-N}, \quad (34)$$

where the superscript (N) stands for the incident parton making N collisions with target partons. From Eq. (31), we have

$$\frac{d\sigma_H^{(N)}}{d\boldsymbol{c}_T}(\boldsymbol{c}_T) = \int \prod_{i=1}^{n} \left(\frac{\alpha_s^2 d\boldsymbol{q}_{iT}}{\boldsymbol{q}_{iT}^4} \right) \delta \left(\boldsymbol{c}_T - \sum_{i=1}^{N} \boldsymbol{q}_{iT} \right). \quad (35)$$

In the sum in Eq. (34), $d\sigma_H^{(N)}/d\boldsymbol{c}_T$ is of order α_s^{2N}. The absorption part is represented by the term $(1 - T\sigma_H)^{A-N}$. We can expand the absorption part $[1 - T(b)\sigma_H]^{A-N}$ as a power series, and we obtain

factor $[1 - T(b)\sigma_H]^{A-N}$. The basic parton-parton collision gives

$$\frac{d\tilde{\sigma}_H^{(1)}}{d\boldsymbol{c}_T}(\boldsymbol{c}_T) \sim \frac{\alpha_s^2}{\boldsymbol{c}_T^4}, \quad (39)$$

where for simplicity a constant coefficient that depends on the nature of the partons as in Eqs. (25) and (27) has been understood. The integrated cross section with a cutoff at p_0 gives

$$\sigma_H^{(1)} \sim \frac{\pi\alpha_s^2}{p_0^2}. \quad (40)$$

We consider the case with $A \gg 1$ in Eq. (38), and we obtain

$$\frac{d\tilde{\sigma}_H^{(2)}(a \rightarrow c)}{d\boldsymbol{c}_T} = 2\left\{ \alpha_s^4 \int_{p_0}^{c_T/2} \left(\frac{d\boldsymbol{q}_{1T}}{\boldsymbol{q}_{1T}^4(\boldsymbol{c}_T - \boldsymbol{q}_{1T})^4} \right) - \frac{d\sigma_H^{(1)}}{d\boldsymbol{c}_T} \sigma_H \right\}. \quad (41)$$

In the integration in the above sum, the dominant contribution comes from the region around $q_{1T} \sim 0$. We expand $1/(\boldsymbol{c}_T - \boldsymbol{q}_{1T})^4$ about $q_{1T} \sim 0$. As a result of the shadowing cancellation in Eqs. (38b) or (39), the singular terms proportional to $1/p_0^6$ cancel out and only a logarithmic

term remains [46]. We find that $d\tilde{\sigma}_H^{(2)}/dc_T$ is given explicitly by

$$\frac{d\tilde{\sigma}_H^{(2)}(a \to c)}{dc_T} = \frac{16\pi\alpha_s^4}{c_T^6} \ln\left\{\frac{c_T}{2p_0}\right\}, \qquad (42)$$

which has a power law $1/c_T^6$ multiplied by a mild logarithm term. Next, we need to study $N = 3$,

$$\frac{d\tilde{\sigma}_H^{(3)}(a \to c)}{dc_T} = \left\{\frac{d\sigma_H^{(3)}}{dc_T} - 3\frac{d\sigma_H^{(1)}}{dc_T}\sigma_H^2\right\}$$
$$- 3\left\{\frac{d\sigma_H^{(2)}}{dc_T} - 2\frac{d\sigma_H^{(1)}}{dc_T}\sigma_H\right\}\sigma_H. \quad (43)$$

We expand $1/(c_T - q_{iT})^4$ again about $q_{iT} \sim 0$. Similarly, the singular terms proportional to $1/p_0^8$ cancel out, and only the logarithmic term remains. We find that $d\tilde{\sigma}_H^{(3)}/dc_T$ is given by

$$\frac{d\tilde{\sigma}_H^{(3)}(a \to c)}{dc_T} = \frac{3\pi^2\alpha_s^6}{c_T^8} \times 312\left[\ln\frac{c_T}{3p_0}\right]^2. \qquad (44)$$

Equations (39), (42), and (44) give explicitly the differential cross sections of a parton after multiple scattering with N scatterer partons as

$$\frac{d\tilde{\sigma}_H^{(N)}(a \to c)}{dc_T} \propto \frac{\alpha_s^{2N}}{c_T^{2+2N}}\left[\ln\frac{c_T}{Np_0}\right]^{N-1}, \qquad (45)$$

which states that the differential cross section for multiple parton scattering obeys a power law with the power index $(2 + 2N)$, multiplied by a logarithm function $[\ln(c_T/Np_0)]^{N-1}$. For the scattering of a parton with one scatterer, it gives α_s^2/p_T^4, with two scatterers it gives $\alpha_s^4 \ln(p_T/2p_0)/p_T^6$, and with three scatterers it gives $\alpha_s^6[\ln(p_T/3p_0)]^2/p_T^8$.

Collecting the terms together, we obtain the differential cross section for the collision of a parton with a composite system with A partons and a thickness function $T(b)$ given by

$$\frac{d\sigma_H^{(\text{tot})}(a \to c)}{dc_T}$$
$$= A\frac{\alpha_s^2}{c_T^4}\int db\, T(b) + \frac{A(A-1)}{2}\frac{16\pi\alpha_s^4}{c_T^6}\ln\left\{\frac{c_T}{2p_0}\right\}$$
$$\times \int db[T(b)]^2 + \frac{A(A-1)(A-2)}{6}\frac{936\pi^2\alpha_s^6}{c_T^8}$$
$$\times \left[\ln\frac{c_T}{3p_0}\right]^2\int db[T(b)]^3. \qquad (46)$$

Depending on the limits of the impact parameter integration, the above result gives the differential cross section for collisions with different centrality selections. For minimum-biased events without an impact parameter selection, one sums over the whole range of impact

parameters. We can consider a thickness function $T(b)$ in the form of a Gaussian given by [19]

$$T(b) = \frac{\exp\{-b^2/2\beta^2\}}{2\pi\beta^2}, \qquad (47)$$

where $\beta = r_0/\sqrt{3}$. (For a proton, $r_0 \sim 0.7$ fm [19].) We then have

$$\int db[T(b)]^N = \frac{1}{N(2\pi\beta^2)^{N-1}}, \qquad (48)$$

and the minimum-biased differential cross section is

$$\frac{d\sigma_H^{(\text{tot})}(a \to c)}{dc_T} = A\frac{\alpha_s^2}{c_T^4} + \frac{A(A-1)}{2}\frac{1}{2(2\pi\beta^2)}\frac{16\pi\alpha_s^4}{c_T^6}\ln\left\{\frac{c_T/2}{p_0}\right\}$$
$$+ \frac{A(A-1)(A-2)}{6}\frac{312}{3(2\pi\beta^2)^2}\frac{3\pi^2\alpha_s^6}{c_T^8}$$
$$\times \left[\ln\frac{c_T}{3p_0}\right]^2. \qquad (49)$$

For another sharp-cutoff thickness function $T(b)$ given by [19],

$$T(b) = \frac{3}{2\pi R^3}\sqrt{R^2 - b^2}\,\Theta(R - b), \qquad (50)$$

we obtain

$$\int db[T(b)]^N = \frac{3^N}{(N+2)2^{N-1}\pi^{N-1}R^{2N-2}}, \qquad (51)$$

and the minimum-biased differential cross section is

$$\frac{d\sigma_H^{(\text{tot})}(a \to c)}{dc_T} = A\frac{\alpha_s^2}{c_T^4} + \frac{A(A-1)}{2}\frac{3^2}{4\times2\pi R^2}\frac{16\pi\alpha_s^4}{c_T^6}$$
$$\times \ln\left\{\frac{c_T/2}{p_0}\right\} + \frac{A(A-1)(A-2)}{6}\frac{3^3312}{5\times2^2\pi^2R^4}$$
$$\times \frac{3\pi^2\alpha_s^6}{c_T^8}\left[\ln\frac{c_T}{3p_0}\right]^2. \qquad (52)$$

Because the power index increases with N as $2 + 2N$, the minimum-biased differential cross section at high c_T in Eqs. (49) or (52) will be dominated by the differential cross section for a single parton-parton $N = 1$ collision, varying as α_s^2/p_T^4.

It should however be recognized that even though the lowest order α_s/c_T^4 dominates at the highest c_T region, contributions of higher order in α_s begin to enter into play under certain circumstances. For example, as the transverse momentum is lowered below the highest c_T region, there will be values of c_T when contributions with higher power index such as $1/c_T^6$ and $1/c_T^8$ in the above series in Eq. (49) or Eq. (52) begin to be important, depending on the value of A, β (or R), and α_s. In another example, as the cone radius R in jet measurements increases, the cone region will contain parton-parton processes with a greater

number of interacting vertices, and it may become necessary to include higher and higher order contributions where contributions of order α_s^{2N} arising from multiple scattering will have a power index $2 + 2N$.

We note in passing that Eq. (47) also gives the centrality dependence of the differential cross section,

$$\frac{d\sigma_H^{(\text{tot})}(a \to c)}{dc_T^2 d\boldsymbol{b}}(c_T, \boldsymbol{b})$$
$$= A\frac{\alpha_s^2}{c_T^4}T(b) + \frac{A(A-1)}{2}\frac{16\pi\alpha_s^4}{c_T^6}\ln\left\{\frac{c_T}{2p_0}\right\}[T(b)]^2$$
$$+ \frac{A(A-1)(A-2)}{6}\frac{936\pi^2\alpha_s^6}{c_T^8}\left[\ln\frac{c_T}{3p_0}\right]^2[T(b)]^3. \quad (53)$$

The above result indicates that one can alter the weights of the different number of scatterers and the power index n, by an impact parameter selection. The number of partons A in a hadron or a nucleus is a dynamical quantity that may depend on the probing transverse momentum and the target nucleus mass number, and it is not yet a well-determined quantity. It is an interesting experimental question whether the numbers of partons A may be so large in some phase space regions or some collision energies as to make it possible to alter the power law behavior of the transverse differential cross section for selected centralities, over different p_T regions. One expects that as the centrality becomes more and more central, contributions with a greater number of multiple parton collisions gains in importance. As a consequence, the power index n is expected to become greater when we select more central collisions.

V. COMPARISON OF A RELATIVISTIC HARD-SCATTERING MODEL WITH EXPERIMENTAL JET TRANSVERSE DIFFERENTIAL CROSS SECTIONS

The results in the last section show that without centrality selection in minimum-biased events, the differential cross section for the production of partons at high-p_T will be dominated by the contribution from a single parton-parton scattering that behaves as α_s^2/c_T^4,

$$\frac{d\sigma_H^{(\text{tot})}(a \to c)}{d\boldsymbol{c}_T} \propto \frac{\alpha_s^2}{c_T^4}, \quad (54)$$

in line with previous analyses on the multiple scattering process in [39–48]. Multiple scatterings with $N > 1$ scatterers contribute to terms of order α_s^{2N} and involve a power law $[\ln(C_T/Np_0)]^{N-1}/c_T^{2+2N}$.

We now consider the lowest order result of Eq. (54). From Eqs. (24) and (54), the relativistic hard scattering cross section of Eq. (24) for the collision of hadrons A and B when a parton a of one of the hadron makes a hard scattering with a partons in the other hadron to produce the parton c is

$$E_p\frac{d^3\sigma(AB \to cX)}{dc^3}$$
$$= \frac{d^3\sigma(AB \to cX)}{dyd\boldsymbol{c}_T}$$
$$\propto \frac{\alpha_s^2(Q^2(c_T^2))(1 - x_{a0}(c_T))^{g_a}(1 - x_{b0}(c_T))^{g_a}}{c_T^4[c_T/\sqrt{s}]^{1/2}}. \quad (55)$$

Different factors in the above equation (55) reveal the physical origins and the associated degrees of freedom. The power law α_s^2/c_T^4 arises from parton-parton hard scattering. The additional $c_T^{1/2}$ in the denominator comes from the $1/\sqrt{\tau_c}$ factor in Eq. (24) and it arises from the integration of the momentum fraction of the other colliding parton x_b. The structure function factor $(1 - x_{a0}(c_T))^{g_a} \times (1 - x_{b0}(c_T))^{g_a}$ comes from the probability for the occurrence of the momentum fractions of the colliding partons. The quantities $x_{a0}(c_T)$ and $x_{b0}(c_T)$ are functions of c_T as given in Eqs. (21) and (22), respectively. The argument c_T inside the structure function factor is the transverse momentum of the scattered parton c, prior to its fragmentation. The exponential indices g_a and g_b come from the structure functions. They can also be estimated from the spectator counting rule of Blankenbecler and Brodsky [15] as given by $g_{\{a,b\}} = 2n_s - 1$, where n_s is the number of spectators of the composite hadron system a or b in the hard-scattering collision. This is essentially the form of the cross section as first suggested by Blankenbecler, Brodsky, and collaborators [15–19].

The results of Eq. (55) can be compared directly with the transverse differential cross sections for hadron jet and isolated photon production. Previously, Arleo *et al.* [21] have presented a method to obtain an ''experimental'' local power index $n^{\text{exp}}(x_c)$. Specifically, referring to Eq. (55) and representing the power index of c_T by n, the lowest order theoretical result of Eq. (55) predicts $n = 4 + 1/2$. One focuses attention at a fixed $x_c(= c_T/\sqrt{s})$ at $\eta = 0$ for which $x_{a0} = x_{b0} = 2x_c$. Upon neglecting the $\sqrt{s}$ dependence of α_s^2, one extracts an experimental power index $n(x_c)$ as a function of x_c by comparing the invariant cross sections at a fixed x_c at different collision energies [21],

$$n(x_c) \sim \frac{\ln[\sigma_{\text{inv}}(\sqrt{s_1}, x_c)/\sigma_{\text{inv}}(\sqrt{s_2}, x_c)]}{\ln[\sqrt{s_2}/\sqrt{s_1}]} + \frac{1}{2}, \quad (56)$$

which is related to the quantity $n^{\text{exp}}(x_c)$ of Arleo *et al.* [21] by $n(x_c) = n^{\text{exp}}(x_c) + 1/2$. Table I summarizes the average experimental power index $\langle n^{\text{exp}} \rangle$ extracted by Arleo *et al.* [21] from the D0 and CDF photon and hadron jet transverse differential cross sections [49–53]. The power indices have the values of $\langle n \rangle = \langle n^{\text{exp}} \rangle + 1/2 = 4.8$–5.2. The local power indices as a function of x_c are also shown in Fig. 2 of Arleo *et al.* [21]. These power indices are in approximate agreement with the power index $n = 4.5$ in Eq. (55) obtained in the relativistic hard-scattering model in perturbative QCD.

TABLE I. The mean power index $\langle n^{\mathrm{exp}} \rangle$ extracted from experimental transverse differential cross sections for hadron and photon jet productions in $p\bar{p}$ collisions at Fermilab as obtained in [21] by comparing the invariant cross sections at different energies.

Collaboration	References	Particles	$\sqrt{s}$ (TeV)	$\langle n^{\mathrm{exp}} \rangle$
CDF	[49]	Hadrons	0.546, 1.8	4.3 ± 0.09
D0	[50]	Hadrons	0.630, 1.8	4.5 ± 0.04
CDF	[51,52]	Photons	0.630, 1.8	4.7 ± 0.09
D0	[53]	Photons	0.630, 1.8	4.5 ± 0.12

As an example to provide a complementary comparison, we focus our attention at a fixed collision energy and express the differential jet cross section $d^3\sigma(AB \to pX)/dyd\mathbf{c}_T$ in Eq. (55) as

$$\frac{d^3\sigma(AB \to cX)}{dyd\mathbf{c}_T}$$
$$= A\frac{\alpha_s^2(Q^2(c_T))(1 - x_{a0}(c_T))^{g_a}(1 - x_{b0}(c_T))^{g_a}}{c_T^n}, \quad (57)$$

where $c_T \sim E_T$, $d\mathbf{c}_T = 2\pi E_T dE_T$. We also use the symbol p_T for the jet transverse momentum c_T. The coupling constant α_s is a function of Q^2, which will be identified as p_T^2. We use the running QCD coupling constant [57],

$$\alpha_s(p_T) = \frac{12\pi}{27\ln(p_T^2/\Lambda_{\mathrm{QCD}}^2)}, \quad (58)$$

where $\Lambda_{\mathrm{QCD}} = 0.25$ GeV has been chosen such that $\alpha_s(M_Z^2) = 0.1184$. We infer from Eq. (57)

$$n = -\frac{d}{d\log p_T}\left\{\log\frac{d\sigma}{d\eta p_T dp_T}\right.$$
$$\left. - \log\left[\alpha_s^2(p_T)(1 - x_{a0}(p_T))^{g_a}(1 - x_{b0}(c_T))^{g_a}\right]\right\}. \quad (59)$$

In the region where $p_T \ll \sqrt{s}$ and the variation of α_s with p_T is not large, the quantity $\log(d\sigma/dyp_T dp_T)$ will be approximately a linear function of $\log p_T$. The log-log plot of $\log(d\sigma/dyp_T dp_T)$ as a function of $\log p_T$ should appear nearly as a straight line, with the power index n given by the magnitude of the slope of the line. In Figs. 3 and 4, the straight lines in the lower E_T regions exhibit such a linear behavior.

We use Eq. (57) to search for the parameters A and n to fit the hadron jet transverse differential cross section as a function of $E_T(\sim p_T)$ at $\eta \sim 0$ in $p\bar{p}$ collisions at Fermilab. The exponential index $g_a = g_b$ for the structure function of a gluon varies from 6 to 10 in different structure functions [58–60]. We shall take $g_a = 6$ from [58]. The experimental D0 hadron jet data of $d\sigma/d\eta E_T dE_T$ at $|\eta| < 0.5$ for $p\bar{p}$ collision at $\sqrt{s} = 1.8$ TeV [50] can be fitted with $n = 4.60$ and $2\pi A = 2.29 \times 10^{15}$ fb GeV^{-2}, as shown in Fig. 3. The experimental D0 hadron jet data of
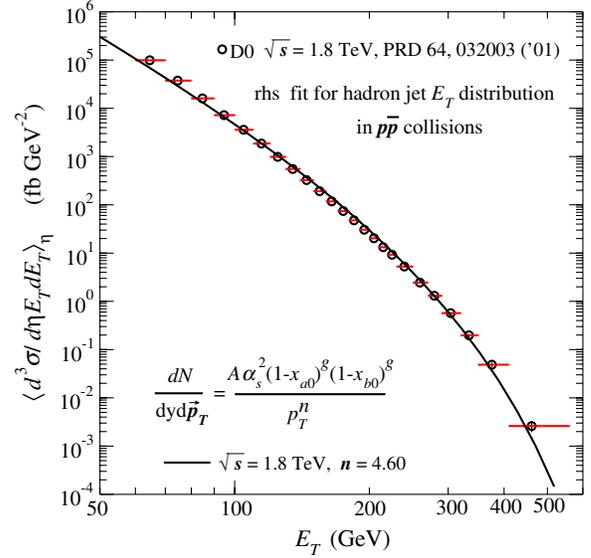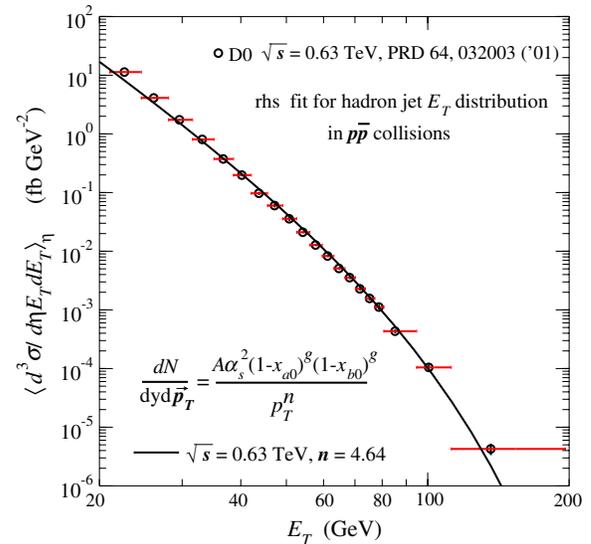

FIG. 3 (color online). Comparison of the experimental $d\sigma/d\eta E_T dE_T$ data from the D0 collaboration [50] for the distribution of hadron jet transverse energy E_T at $|\eta| < 0.5$, in $p\bar{p}$ collision at $\sqrt{s} = 1.8$ TeV, with the relativistic hard-scattering model result in Eq. (57).

$d\sigma/d\eta E_T dE_T$ for $p\bar{p}$ collision at $\sqrt{s} = 0.630$ TeV [50] can be fitted with $n = 4.64$ and $2\pi A = 1.64 \times 10^9$ fb GeV^{-2}, as shown in Fig. 4. These power indices are in approximate agreement with the value of $n = 4.5$ in Eq. (55), indicating the approximate validity of the hard-scattering model description for jet production in hadron-hadron collisions, with the predominant α_s^2/c_T^4 parton-parton

FIG. 4 (color online). Comparison of the experimental $d\sigma/d\eta E_T dE_T$ data from the D0 collaboration [50] for the distribution of hadron jet transverse energy E_T at $|\eta| < 0.5$, in $p\bar{p}$ collision at $\sqrt{s} = 0.630$ TeV, with the relativistic hard-scattering model result in Eq. (57).
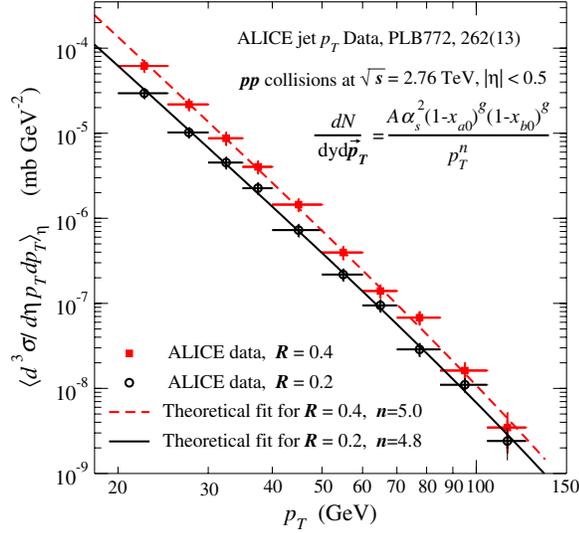
FIG. 5 (color online). Comparison of the experimental $d\sigma/d\eta p_T dp_T$ data from the ALICE collaboration [61] for the transverse momentum distribution of hadron jets $d\sigma/d\eta p_T dp_T$ at $|\eta| < 0.5$, in pp collision at $\sqrt{s} = 2.76$ TeV, with the relativistic hard-scattering model result in Eq. (57).
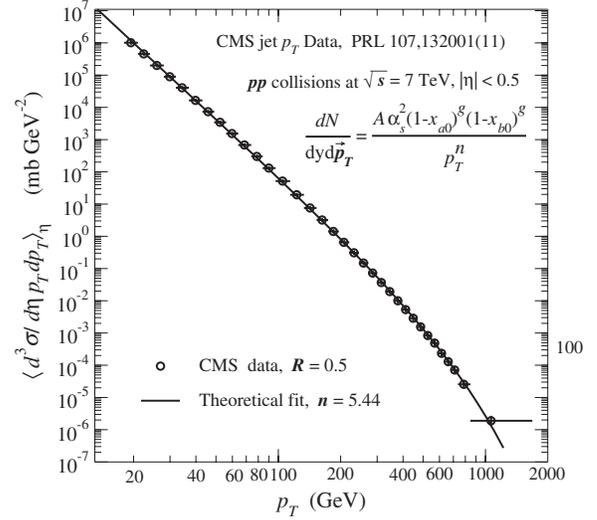

FIG. 6. Comparison of the experimental $d\sigma/d\eta p_T dp_T$ data from the CMS collaboration [67] for the transverse momentum distribution of hadron jets $d\sigma/d\eta p_T dp_T$ at $|\eta| < 0.5$, in pp collision at $\sqrt{s} = 7$ TeV, with the relativistic hard-scattering model result in Eq. (57).

differential cross section. These power indices extracted from the differential cross section are also in approximate agreement with those in Table I extracted by comparing cross sections at two different energies [21].

In another comparison of the jet production data with the hard-scattering model, we examine in Fig. 5 the jet differential cross section $d\sigma/d\eta p_T dp_T$ in pp collisions at $\sqrt{s} = 2.76$ TeV at the LHC obtained by the ALICE collaboration at $\eta < 0.5$ with $R = 0.4$ and 0.2 [61]. The log-log plot of $\log[d\sigma/d\eta p_T dp_T]$ versus $\log p_T$ gives nearly a straight line with the slope $-n$. The jet differential cross section can be fitted with the power index $n = 5.0 \pm 0.2$ and an overall magnitude of $2\pi A = 2080$ mb GeV^{-2} for $R = 0.4$ and $n = 4.8 \pm 0.2$ and an overall magnitude of $2\pi A = 535$ mb GeV^{-2}. These power indices are close to the value of $n = 4.5$ expected in Eq. (55) in the hard-scattering model.

In another comparison, we show in Fig. 6 the jet differential cross section $d\sigma/d\eta p_T dp_T$ in pp collisions at $\sqrt{s} = 7$ TeV at the LHC obtained by the CMS collaboration at $\eta < 0.5$ with $R = 0.5$ [27]. The jet differential cross section can be fitted with the power index $n = 5.44 \pm 0.1$ and of $2\pi A = 5.05 \times 10^{14}$ mb GeV^{-2} as shown in Fig. 7. The value of n is slightly greater than the expected value of $n = 4.5$.

We note in the last few examples that the power index n increases slightly as the cone radius R increases. An increase in the cone radius allows the sampling of events with a greater number of the parton-parton interaction vertices inside the cone, and each interaction vertex brings in a power of α_s^2. A greater cone radius has greater contributions from processes that are higher order in α_s. Thus,

among many high next-to-leading order and next-to-next-to-leading order contributions, some of the α_s^4/p_T^6 contributions of the multiple scattering processes discussed in Eqs. (49) and (52) in Secs. III and IV may also need to be included. Because of the limited number of cases, more measurements will be needed to confirm whether the increase in the power index with increasing R is a general phenomenon.
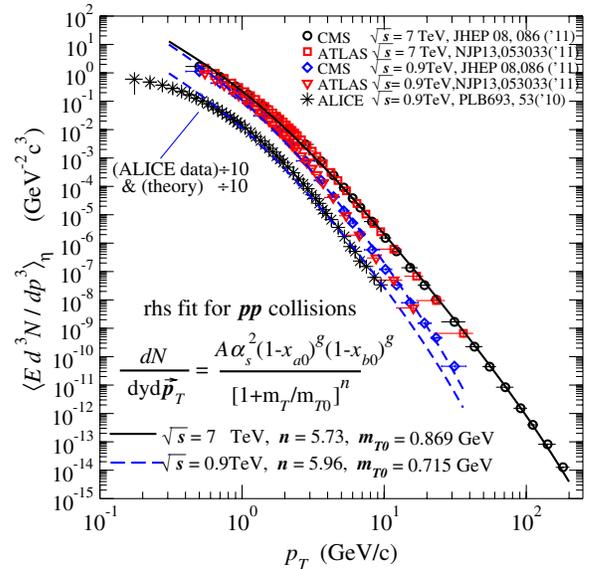

FIG. 7 (color online). Comparison of the experimental transverse momentum distribution $\langle E_p d^3N/dp^3 \rangle_\eta$ of hadrons in pp collisions with the relativistic hard-scattering model, Eq. (85), assuming a linear m_T dependence of the regulating function.

We conclude from these comparisons of the transverse differential cross sections of hadron jets in both $p\bar{p}$ and pp collisions at high energies that the data supports the relativistic hard-scattering description of the collision process, with a basic parton-parton differential cross section behaving approximately as α_s^2/p_T^4 with some tentative evidence of an increase in the power index as R increases.

It is interesting to note that when the structure function information is known from other measurements, the hadron jet spectra differential cross section can be reasonably described with only a single power index n and an overall magnitude parameter A. The shape of the transverse differential cross section of hadron jets has only a very small number of the degrees of freedom.

VI. EFFECTS OF FRAGMENTATION ON TRANSVERSE DIFFERENTIAL CROSS SECTION

Experimentally, we detect hadrons and the construction of a hadron jet is inferred from a correlated cone of hadrons. Experimental measurements also give hadron spectra at high transverse momenta without reconstructing jets. The analyses of the power indices n give $n \sim 7$ for hadron transverse spectra [33] but $n = 4.5$–5 for jet transverse differential cross sections as shown in the last section. The difference between the power indices is likely to arise from the subsequent evolution of the parton.

Other pieces of evidence that the parton-to-hadron final-state evolution may lead to a change in the power index show up when we compare the experimental local power indices for jets and for hadrons [21]. In Fig. 2 of Ref. [21], the local power indices $n^{\exp}$ as a function of $x_\perp = 2x_c$ cluster around $n^{\exp} \sim 4.5$ for jets but $n^{\exp} \sim 5$–9 for hadrons. Furthermore, Table I of [21] gives $\langle n^{\exp} \rangle$ for jets that are substantially smaller than $\langle n^{\exp} \rangle$ for hadrons. We need to consider the difference between jets and hadrons and the fragmentation and showering of jets (representing partons) to become hadrons.

We shall view the parton fragmentation and the accompanying showering as equivalently final-state processes and speak of them interchangeably to emphasize different aspects of the parton final-state evolution. In the remaining sections, we shall consistently use the symbol c to label a parton and its momentum and the symbol p to label a hadron and its momentum.

In the showering of a parton c, a large number of hadrons comes out nearly collinearly with the parton c in a cone along the $\boldsymbol{c}$ direction. In the present study of high-p_T particles in the central rapidity region, the parton c is predominantly along the transverse direction, and the shower of the produced hadrons will also be along the transverse direction. For the study of the high-p_T spectra as a result of the showering of a parton c, it suffices to focus attention on the leading hadron p of the cone of shower particles, because of the rapid falloff of the transverse momentum distribution as a function of increasing c_T.

The leading hadron fragment with transverse momentum p_T contributes significantly to the final spectra at that p_T whereas nonleading hadron fragments of the shower contribute only insignificantly to the spectra at their corresponding p_T values. Thus, for the examination of the high-p_T hadron spectra after parton fragmentation and showering, each parent parton c with a momentum c_T can be viewed as fragmenting into a single leading hadron p with momentum p_T by the showering process.

The showering of the partons will go over many generations of branching and each branching will degrade the momentum of the showering parton by a momentum fraction ζ. We can consider the transverse momentum p_T of the leading hadron as arising from the λth branching generation of the shower. The 4-momentum of the leading hadron p and the 4-momentum of the parent parton c are related by

$$p = \zeta^\lambda c. \tag{60}$$

We relabel the cumulative product ζ^λ by the momentum fraction z,

$$z = \zeta^\lambda, \tag{61}$$

to relate p with c,

$$p = zc. \tag{62}$$

The probability for the fragmentation of the parton c into the hadron p is specified phenomenologically by the fragmentation function $D_{p/c}(z)$, which depends on the QCD momentum transfer scale.

We shall consider first the simplest case of showering and fragmentation in which the momentum fraction z is independent of the magnitude of the parton transverse momentum c_T. We shall consider a more sophisticated showering algorithm in the next section. In this case with z independent of c_T, the hadron transverse momentum p_T is a linear function of the parton transverse momentum c_T in Eq. (62). Under the fragmentation from the parton c to the hadron p, the differential cross sections $d\sigma(AB \to pX)/dp^4$ and $d\sigma(AB \to cX)/dc^4$ are related by

$$\frac{d\sigma(AB \to pX)}{dp^4} = \int dz D_{p/c}(z)$$
$$\times \int dc^4 \frac{d\sigma(AB \to cX)}{dc^4} \delta^{(4)}(p - zc). \tag{63}$$

We therefore have

$$E_p \frac{d\sigma(AB \to pX)}{dp^3} = \frac{d\sigma(AB \to pX)}{dy d\boldsymbol{p}_T}$$
$$\propto \int \frac{dz}{z^2} D_{p/c}(z) z^{4+1/2}$$
$$\times \frac{\alpha_s^2(c_T)(1 - x_{a0}(c_T))^{g_a}(1 - x_{b0}(c_T))^{g_a}}{p_T^{4+1/2}}, \tag{64}$$

where the arguments c_T in x_{a0} and x_{b0} are evaluated at $c_T = p_T/z$. We can expand the factor $\alpha_s(c_T) \times (1 - x_{a0}(c_T))^{g_a} (1 - x_{b0}(c_T))^{g_a}$ about $\bar{c}_T$ in the above equation as a power series of c_T,

$$f(c_T) = \alpha_s(c_T)((1 - x_{a0}(c_T))^{g_a}(1 - x_{b0}(c_T))^{g_b}$$
$$= f(\bar{c}_T) + (c_T - \bar{c}_T)f'(c_T) + \frac{(c_T - \bar{c}_T)^2}{2}f''(c_T). \tag{65}$$

The error in the first order is minimized if $\bar{c}_T$ is defined as

$$\bar{c}_T = \left\langle \frac{p_T}{z} \right\rangle = p_T \left\langle \frac{1}{z} \right\rangle, \tag{66}$$

where

$$\left\langle \frac{1}{z} \right\rangle = \frac{\int dz \frac{1}{z^2} D_{p/c}(z) z^{4+1/2} \frac{1}{z}}{\int dz \frac{1}{z^2} D_{p/c}(z) z^{4+1/2}}. \tag{67}$$

We can obtain the magnitude of $\langle 1/z \rangle$ by using the fragmentation function from Ref. [62] for a parton to fragment into a pion for $Q_0^2 = 2$ GeV^2,

$$D_{\pi/q}(z) = 0.551 z^{-1}(1 - z)^{1.2}, \quad D_{\pi/g}(z) = 3.77(1 - z)^2.$$

We find

$$\bar{c}_T = p_T \left\langle \frac{1}{z} \right\rangle = \begin{cases} 2.2 p_T, & \text{for a gluon parton,} \\ 2.46 p_T, & \text{for a quark parton.} \end{cases} \tag{68}$$

For our numerical work, we shall use the average value for gluon and quark partons,

$$\bar{c}_T = p_T \left\langle \frac{1}{z} \right\rangle = 2.33 p_T. \tag{69}$$

The differential cross section $d\sigma(AB \to pX)/dy d\boldsymbol{p}_T$ of Eq. (64) for the hard scattering of hadrons A and B after fragmenting (and showering) to hadron p can be approximated by

$$\frac{d\sigma(AB \to pX)}{dy d\boldsymbol{p}_T} \propto \frac{\alpha_s^2(\bar{c}_T)(1 - x_{a0}(\bar{c}_T))^{g_a}(1 - x_{b0}(\bar{c}_T))^{g_a}}{p_T^{4+1/2}}, \tag{70}$$

where $\bar{c}_T$ is given by Eq. (69).

VII. PARTON SHOWERING AND THE POWER INDEX n

The results of the last section indicate that with a fragmentation fraction z that is independent of the fragmentation parton momentum c_T in the showering process, the power law and the power index are unchanged, and the power index $n + 1/2$ for the produced hadrons should be approximately 4.5 as given by Eq. (55) or Eq. (70). On the other hand, the transverse spectra of produced hadrons in high-energy pp collisions at the LHC gives a power index $n \sim 7$ [21,27–30,33]. Theoretically, the PYTHIA program

with additional parton showering and radiations can describe quite well the transverse momentum distributions of produced hadrons in pp collisions at LHC energies [27], which are associated with a power index $n \sim 7$ [33]. The difference between the power index of $n \sim 4$–5 from the transverse differential cross sections of hadron and photon jets and $n \sim 7$ from the transverse spectra of hadrons is likely to arise from the subsequent showering of the parton jets to hadron fragments of lower transverse momenta.

It should be realized that the showering mechanism presented in the last section may not contain sufficient degrees of freedom to describe properly the QCD showering process. In addition to the kinematic decrease of the magnitude of the transverse momentum as governed by Eq. (62),

$$\frac{p_T}{c_T} = \zeta^\lambda, \tag{71}$$

the showering is governed by an additional criterion on the virtuality, which measures the degree of the off-the-mass-shell property of the parton. There are three different parton showering schemes: the PYTHIA [63], the HERWIG [64], and the ARIADNE [65]. The general picture is that the initial parton with a large initial virtuality Q decreases its virtuality by showering until a limit of Q_0 is reached. Each of the three schemes uses a different relation between the virtuality and the attributes of the showering parton, and each with a different evolution variable and a different virtuality limit. Their kinematical schemes, the treatments of soft gluon interference, and the hadronization schemes are also different.

We can abstract from these different parton showering schemes to infer that there is approximately a one-to-one mapping of the initial virtuality Q with the transverse momentum c_T of the evolving parton as showering proceeds. The initial virtuality Q scales with, and maps into, the initial transverse c_T of the showering parton, and the cutoff virtuality Q_0 scales with, and maps into, a transverse momentum p_{T0} of the parton. In each successive generation of the showering, the virtuality decreases by a virtuality fraction which corresponds, in terms of the corresponding mapped parton transverse momentum, to a decrease by a transverse momentum fraction $\tilde{\zeta}$. The showering will end in λ generations such that

$$\frac{p_{T0}}{c_T} = a\tilde{\zeta}^\lambda, \tag{72}$$

where a is a constant relating the scales of virtuality and transverse momentum. Thus, the showering process depends on the magnitude of c_T and the limiting virtuality Q_0, which corresponds to a parton momentum p_{T0}. The greater the value of c_T, the greater the number of generations λ. We can infer an approximate relation between c_T and the number of generations λ,

$$\lambda = \ln \frac{p_{T0}}{ac_T} / \ln \tilde{\zeta}. \tag{73}$$

On the other hand, kinematically, the showering processes degrade the transverse momentum of the parton c_T to that of the hadron p_T as given by Eq. (71), depending on the number of generations λ. The magnitude of the hadron transverse momentum p_T is related (on the average) to the parton transverse momentum c_T by

$$\frac{p_T}{c_T} = \zeta^\lambda = \zeta^{\ln \frac{p_{T0}}{ac_T}/\ln \tilde{\zeta}}. \tag{74}$$

We can solve the above equation for p_T as a function of c_T,

$$\frac{p_T}{p_{T0}} = \left(\frac{c_T}{p_{T0}}\right)^{1-\mu} a^{-\mu}, \tag{75}$$

and alternatively for c_T as a function of p_T,

$$\frac{c_T}{p_{T0}} = \left(\frac{p_T}{p_{T0}}\right)^{1/(1-\mu)} a^{\frac{\mu}{1-\mu}}, \tag{76}$$

where

$$\mu = \ln \zeta / \ln \tilde{\zeta} > 0, \tag{77}$$

and μ is a parameter that can be searched to fit the data. As a result of the virtuality ordering and virtuality cutoff, the hadron fragment transverse momentum p_T is related to the parton momentum c_T by an exponent $1 - \mu$.

After the fragmentation and showering of the parton c to hadron p, the hard-scattering cross section for the scattering in terms of hadron momentum p_T becomes

$$\frac{d^3\sigma(AB \to pX)}{dyd\mathbf{p}_T} = \frac{d^3\sigma(AB \to cX)}{dyd\mathbf{c}_T}\frac{d\mathbf{c}_T}{d\mathbf{p}_T}$$
$$\propto \frac{\alpha_s^2(\bar{c}_T)(1 - x_{a0}(\bar{c}_T))^{g_a}(1 - x_{b0}(\bar{c}_T))^{g_a}}{c_T^{4+1/2}}\frac{d\mathbf{c}_T}{d\mathbf{p}_T}. \tag{78}$$

From the relation between the parent parton moment c_T and the leading hadron p_T in Eq. (76), we get

$$\frac{d\mathbf{c}_T}{d\mathbf{p}_T} = \frac{1}{1-\mu}\left(\frac{p_T}{p_{T0}}\right)^{\frac{2\mu}{1-\mu}} a^{\frac{2\mu}{1-\mu}}. \tag{79}$$

Therefore under the fragmentation from c to p, the hard-scattering cross section for $AB \to pX$ becomes

$$\frac{d^3\sigma(AB \to pX)}{dyd\mathbf{p}_T} \propto \frac{\alpha_s^2(\bar{c}_T)(1 - x_{a0}(\bar{c}_T))^{g_a}(1 - x_{b0}(\bar{c}_T))^{g_a}}{p_T^{n'}}, \tag{80}$$

where

$$n' = \frac{n - 2\mu}{1 - \mu}, \quad \text{with} \quad n = 4 + \frac{1}{2}. \tag{81}$$

Thus, from Eqs. (76)–(79), the parton showering process with limiting virtuality may modify the power law index in the transverse differential cross section from n to n'. The parameter μ is related to n and n' by

$$\mu = \frac{n' - n}{n' - 2}. \tag{82}$$

VIII. PHENOMENOLOGICAL MODIFICATIONS OF THE HARD-SCATTERING CROSS SECTION

In the last section we give qualitative arguments to show that the power index may be modified from n to n' by the process of showering. A quantitative evaluation of the changes in the power index from fundamental QCD principles is difficult, because the showering and the subsequent hadronization processes are complicated and contain unknown nonperturbative elements. It suffices to verify that there is indeed a systematic change of the power index from partons (or their equivalent representative jets) to hadrons, by finding the empirical values of power index n for hadron production. For such a purpose, we shall modify the differential cross section $d^3\sigma(AB \to pX)/dyd\mathbf{p}_T$ in (80), for an incident parton a scattering into c after a relativistic hard scattering, showering, and hadronization to be

$$\frac{d^3\sigma(AB \to pX)}{dyd\mathbf{p}_T} \propto \frac{\alpha_s^2(\bar{c}_T)(1 - x_{a0}(\bar{c}_T))^{g_a}(1 - x_{b0}(\bar{c}_T))^{g_a}}{[1 + m_T/m_{T0}]^n}, \tag{83}$$

where m_T is the transverse mass $\sqrt{m^2 + p_T^2}$ of the detected hadron p, and m is the hadron mass taken to be the pion mass. The transverse mass m_{T0} has been introduced both to regulate the behavior of the cross section in the region of small p_T and to represent the average transverse mass of the detected hadron in the hard-scattering process. Experiments measure the differential yield in nonsingle-diffractive events, which is related to the differential cross section by

$$E_p\frac{d^3N(AB \to pX)}{dp^3} = E_p\frac{d^3\sigma(AB \to pX)}{\sigma_{\text{NSD}}dp^3}, \tag{84}$$

where σ_{NSD} is the nonsingle-diffractive cross section. We also need to transcribe the invariant cross section in terms of $d\sigma/d\eta d\mathbf{p}_T$. We have then the produced particle distribution

$$\frac{d^3N(AB \to pX)}{d\eta d\mathbf{p}_T} = \sqrt{1 - \frac{m^2}{m_T^2 \cosh^2 y}} A \frac{\alpha_s^2(\bar{c}_T)(1 - x_{a0}(\bar{c}_T))^{g_a}(1 - x_{b0}(\bar{c}_T))^{g_b}}{[1 + m_T/m_{T0}]^n}, \tag{85}$$

where A is a constant fitting parameter. We shall use the above formula, Eq. (85), to search for the power index n for hadron production by fitting the hadron transverse momentum distributions in pp collisions at the LHC from the CMS [28], ATLAS [29], and ALICE collaborations [30], within the experimental pseudorapidity windows. We shall again take $g_a = g_b = 6$ [58]. In Fig. 6, we compare the fits to the experimental hadron transverse spectra. We find that for pp collisions at $\sqrt{s} = 7$ TeV, the parameters are $n = 5.73$, $m_{T0} = 0.869$ GeV, and $A = 194$ GeV^{-2} c^3, and for pp collisions at $\sqrt{s} = 0.9$ TeV, the parameters are $n = 5.96$, and $m_{T0} = 0.715$ GeV, $A = 236$ GeV^{-2} c^3.

Note that if we introduce

$$q = 1 + \frac{1}{n} \quad \text{and} \quad T = \frac{m_{T0}}{q-1}, \tag{86}$$

then we get

$$\frac{d^3 N(AB \to pX)}{d\eta dp_T}$$
$$= \sqrt{1 - \frac{m^2}{m_T^2 \cosh^2 y}} A\alpha_s^2(\bar{c}_T)(1 - x_{a0}(\bar{c}_T))^{g_a}$$
$$\times (1 - x_{b0}(\bar{c}_T))^{g_b} \left[1 - (1-q)\frac{m_T}{T} \right]^{\frac{1}{1-q}}, \tag{87}$$

$$\frac{d^3 N(AB \to pX)}{d\eta dp_T} = \sqrt{1 - \frac{m^2}{m_T^2 \cosh^2 y}} A \frac{\alpha_s^2(\bar{c}_T)(1 - x_{a0}(\bar{c}_T))^{g_a}(1 - x_{b0}(\bar{c}_T))^{g_b}}{[1 + m_T^2/m_{T0}^2]^{n/2}}. \tag{89}$$

which is in the form of the Tsallis distribution of Eq. (1) (now with a clear meaning of the "nonextensivity parameter" q and the "temperature" T as given in Eq. (86)). The difference is the additional p_T dependencies of $\alpha_s^2(\bar{c}_T)$, $x_{a0}(\bar{c}_T)$, $x_{b0}(\bar{c}_T)$ as well as the square-root prefactor. What needs to be stressed is that the real active number of degrees of freedom remains quite small, similar to Eq. (1).

Equation (83) is not the only way we can parametrize the hard-scattering results. The gluon exchange propagator in the Feynman diagrams of Figs. 1 and 2 and Eqs. (31) and (35) involve the quantities q_{Ti}^2. We can alternatively modify the basic differential cross section $d^3 \sigma(AB \to pX)/dyd\boldsymbol{p}_T$ for the scattering of a to p in the quadratic m_T^2 form,

$$\frac{d^3 \sigma(AB \to pX)}{dyd\boldsymbol{p}_T} \propto \frac{\alpha_s^2(\bar{c}_T)(1 - x_{a0}(\bar{c}_T))^{g_a}(1 - x_{b0}(\bar{c}_T))^{g_a}}{[1 + m_T^2/m_{T0}^2]^{n/2}}. \tag{88}$$

With such an effective representation of the basic $a \to p$ scattering, Eq. (80) is altered to become

We use the above equation with the quadratic m_T^2 dependence in the transverse distribution to search the power index n by fitting the experimental hadron transverse momentum distribution $\langle E_p d^3 N/dp^3 \rangle_\eta$ in pp collisions from the CMS [28], ATLAS [29], and ALICE collaborations [30]. The data for $p_T \gtrsim 0.5$ GeV/c agree with the theoretical fits as shown in Fig. 8. The parameters for pp collisions at $\sqrt{s} = 7$ TeV are $n = 5.83$, $m_{T0} = 0.856$ GeV, and $A = 3.58$ GeV^{-2} c^3, and for pp collisions at $\sqrt{s} = 0.9$ TeV, the parameters are $n = 5.97$, $m_{T0} = 0.685$ GeV, and $A = 4.58$ GeV^{-2} c^3. We give the fitting parameters that describe the p_T contributions from spectra at the two different energies in Table II.

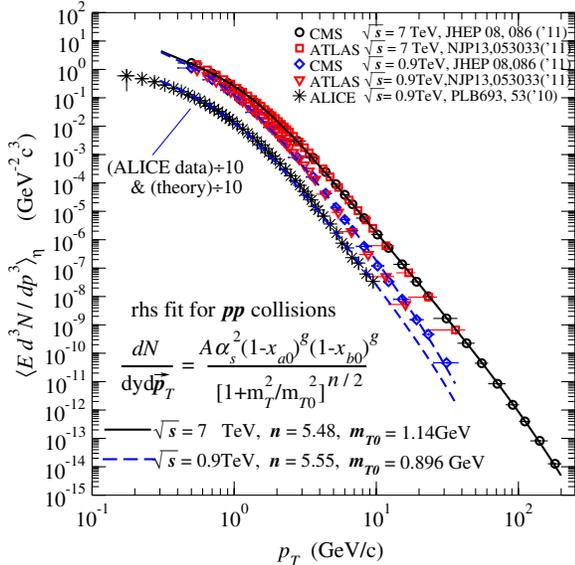FIG. 8 (color online). Comparison of the experimental hadron transverse momentum distribution $\langle E_p d^3 N/dp^3 \rangle_\eta$ of hadrons in pp collisions with the relativistic hard-scattering model, Eq. (85), assuming a quadratic m_T dependence of the regulating function.

TABLE II. Fitting parameters n, m_{T0}, and A for the transverse momentum distribution of hadrons in pp collisions.

| | Linear m_T Eq. (85) | | Quadratic m_T^2 Eq. (89) | |
	$\sqrt{s} = 7$ TeV	$\sqrt{s} = 0.9$ TeV	$\sqrt{s} = 7$ TeV	$\sqrt{s} = 0.9$ TeV
n	5.73	5.96	5.48	5.55
m_{T0} (GeV)	0.869	0.715	1.14	0.896
A (GeV^{-2} c^3)	194	236	12.8	13.8

Comparing the results from the two different ways of expressing the power-law behaviors, we find that the agreements of the data with the theoretical curves are nearly the same above $p_T \gtrsim 3$ GeV/c, but the theoretical results for the linear case with the m_T dependence of Eq. (85) are less than the experimental ALICE data for $p_T \sim 2$ GeV/c but greater than the experimental data for $p_T \lesssim 0.5$ GeV/c. On the other hand, the quadratic m_T^2 expression of Eq. (89), that is a more natural from field theory point of view involving gluon propagators, leads to a better agreement in the lower p_T region.

For pp collisions at the LHC, the above comparisons indicate that the power index extracted from hadron spectra has the value of $n \sim 6$. The power index is systematically larger than the power index of $n \sim 4$–5 extracted from jet transverse differential cross sections. Considering the difference of a jet and hadrons, we can infer that the process of fragmentation and showering increases the value of the power index n of the transverse spectra.

It should be noted that the hard-scattering model results in the low-p_T region will be slightly modified with the introduction of the intrinsic p_T of the partons [54]. There will also be modifications due to the recombination of partons [5]. Nevertheless, the extrapolation of the hard-scattering results to the low-p_T region as obtained here indicates indeed that the hard-scattering process can contribute substantially to the production of particles at the low-p_T region[4] as has been suggested by Trainor and collaborators [24].

IX. DISCUSSIONS AND CONCLUSIONS

We have been stimulated by the good agreement of the Tsallis distribution with the transverse momentum distribution of produced hadrons over a large range of the transverse memorandum in pp collisions at LHC energies. The simplicity of the Tsallis distributions raises questions on the physical meaning of the few degrees of freedom entering into the Tsallis distribution.

As the magnitude of the transverse momentum in this high-p_T region is much greater than the mean transverse momentum, concepts such as statistical mechanics that depend on thermodynamical equilibrium or quasiequilibrium may be subject to question. The asymmetry between the transverse and the longitudinal degrees of freedom also poses additional difficulties in a statistical explanation of the full three-dimensional momentum distribution in this high-p_T region.

We therefore attempt to understand the results of a simple Tsallis fit of the transverse momentum distribution in pp collisions within the relativistic hard-scattering

---

[4]Note that, for example, for $q \neq 1$ the normalization of the rapidity distribution given by Eq. (87) depends on q.

model. The relativistic hard-scattering model however predicts that the differential cross section for the production of high-p_T particles should vary as $1/p_T^n$ with $n = 4$ if the basic process consists of elementary parton-parton $2 \rightarrow 2$ processes. The Tsallis fit to the LHC data gives a power index for hadrons of $n \sim 7$ that is substantially greater.

Our reexamination of the relativistic hard-scattering model reveals that for minimum biased events without a centrality selection, the differential cross section at high p_T is dominated by the contribution from a single parton-parton collision with the α_s^2/c_T^4 behavior. The multiple scattering process leads to contributions of higher power indices that will not modify significantly the α_s^2/c_T^4 behavior at high p_T. The power index n should be approximately $4 + 1/2$ where the additional power of $1/2$ arises from the integration of the structure function. Indeed, comparison with the experimental power indices in the transverse differential cross sections for jet production supports the approximate validity of a basic α_s^2/c_T^4 behavior for parton-parton collisions in relativistic hard-scattering processes.

As a hadron jet or a photon jet corresponds to the state of a parton after a parton-parton collision but before the final-state showering, we now understand that the systematic difference between the power index of $n \sim 4$–5 for jets [21,49–53,61], and $n \sim 6$–7 for hadrons [33] may be attributed to the subsequent showering and hadronization of the parton jet to hadron fragments of lower transverse momenta. Another part of the increase of the power index arises from the p_T dependence of the structure function factor $(1 - x_{a0})^g (1 - x_{b0})^g$ and the running coupling constant.

While we examine here the contributions of the hard processes, there can also be contributions of the produced particles from soft processes in the low-p_T region. These contributions relative to those from hard processes will certainly diminish as the collision energy increases. It is therefore entirely possible that the borderline between soft and hard processes moves to the lower p_T region as the collision energy increases. How the borderline between the two processes can be determined will require much more future work.

Many relevant questions on the borderline between the high-p_T and the low-p_T regions will need to be settled in the future. First, it is expected that hard-scattering processes will be accompanied by collisional correlations different from those from soft processes. A careful analysis of the two-particle correlations in the low-p_T region may provide a way of separating out the soft process contributions from the hard-scattering collisional contributions in the low-p_T region [24]. Second, while we apply the relativistic hard-scattering model to the low-p_T region of $p_T \lesssim 2$ GeV/c, the approximations we have used may not have its range of validity down to such regions.

The establishment of the low-p_T limit of validity of the relativistic hard-scattering model will be both an experimental and theoretical question. Processes such as parton intrinsic transverse momentum [54] and parton recombination [5] will add complexity to the transverse momentum distribution in the low-p_T region. Third, the separation of the soft process contribution and the knowledge of the borderline between the soft processes and the hard processes may also provide information whether the basic collision law should be represented by a linear form of m_T in Eq. (85) or a quadratic form of m_T^2 in Eq. (89).

The low-p_T region is conventionally associated with soft nonperturbative processes and the high-p_T region with perturbative hard-scattering processes. A very different two-component model (TCM) scheme for partitioning the soft and hard components has been proposed [23,24]. Measurements of the STAR collaboration [23] on the transverse distribution $d^3N/d\eta dp_T^2$ around $\eta \sim 0$, as a function of the event multiplicity classes, reveal that the distribution $d^3N/d\eta dp_T^2$ can be approximately written as the sum of a term linear in multiplicity, $n_{\mathrm{ch}}S_0(p_T)$, and a term quadratic in multiplicity, $n_{\mathrm{ch}}^2 H_0(p_T)$ [23]. Under the hypothesis that the multiplicity of hard collisions n_h is proportional to n_{ch}^2 while the multiplicity of soft collisions n_s is linear in n_{ch}, the $S_0(p_T)$ contribution, parametrized in the Levy form or the equivalent Tsallis form as a function of p_T, $S_0(p_T) \sim 1/[1 + (m_T - m_0)/nT]^n$, is identified in the TCM scheme as the TCM "soft" component, and the $H_0(p_T)$ contribution, parametrized as a Gaussian in shifted $y_T = \ln[(m_T + p_T)/m]$, is identified as the TCM "hard" component [23,24]. As a result of such a partition, the TCM soft component remains significant even at very high p_T and contains a power law $1/p_T^n$ behavior, which however occurs only in the conventional hard component of the relativistic hard-scattering model. On the other hand, the TCM hard component is a Gaussian distribution in shifted y_T centered at $p_T \sim 1.4$ GeV and it does not have the power-law behavior of the relativistic hard scattering model at high p_T. The TCM partitions are in variance with those in our physical, and conventional partitions. As there are many different ways of partitioning the spectrum, the theoretical, physical, and mathematical basis for the two-component model partition in the form as presented as soft and hard in [23,24] may need to be further investigated.

Returning to the Tsallis distribution which motivates the present investigation, we can conclude that the successes of representing the transverse spectra at high-p_T by a Tsallis distribution arise from (i) the simple power-law behavior of the parton-parton scattering cross section, α_s^2/c_T^4, with a power index of 4, and (ii) the few

number of the degrees of freedom in the hard-scattering model. The power index of 4 has been found experimentally to be approximately valid by examining the differential cross sections of hadron jets and photon jets. It has also been found theoretically to be approximately valid by examining the multiple scattering process. The power index is not significantly modified by the multiple scattering process in minimum biased measurements. The α_s^2/p_T^4 power law lays the foundation for Tsallis/Hegedorn-type transverse momentum distributions, and the few degrees of freedom in the Tsallis distribution is a reflection of the few degrees of freedom in the underlying hard-scattering model. There is additional p_T dependence due to the parton structure function, the running coupling constant, and the parton momentum integration, which lead to a slightly larger power index. Furthermore, in going from the parton measurements in terms of jets to hadron measurements in terms of fragmented hadron products, there are additional showering and fragmentation processes which give rise to a greater value of the power index. The Tsallis distribution is flexible enough to adjust the power index to accommodate the different and changing environment, yielding a nonstatistical description of the distribution.

Because of its nonstatistical nature, the parameters in a Tsallis distribution can only be supplied and suggested from nonstatistical means, such as the QCD basic parton-parton scattering power index and the QCD multiple scattering shadowing effects. It also is limited in its application to the transverse degree of freedom, as there is no way to generalize the Tsallis parameters across the three-dimensional space from transverse to longitudinal coordinates. For a more fundamental description, it is necessary to turn to the basic parton model for answers. For example, the relativistic hard scattering can be applied to collision to other longitudinal regions of pseudorapidities where in the forward rapidity region, the additional mechanism of direct fragmentation [66] should also be included. The underlying relativistic hard-scattering model has a greater range of applications and a stronger theoretical foundation.

[1] G. Gatoff and C.-Y. Wong, Phys. Rev. D **46**, 997 (1992); C.-Y. Wong and G. Gatoff, Phys. Rep. **242**, 489 (1994).

[2] R. Hagedorn, Riv. Nuovo Cimento **6**, 1 (1983).

[3] R. Hagedorn and K. Redlich, Z. Phys. C **27**, 541 (1985).

[4] I. Kraus, J. Cleymans, H. Oeschler, and K. Redlich, Phys. Rev. C **79**, 014901 (2009).

[5] R. C. Hwa and C. B. Yang, Phys. Rev. C **67**, 034902 (2003); R. C. Hwa and Z. G. Tan, Phys. Rev. C **72**, 057902 (2005); R. C. Hwa and C. B. Yang, Phys. Rev. C **75**, 054904 (2007); C. B. Chiu and R. C. Hwa, Phys. Rev. C **72**, 034903 (2005); R. C. Hwa, Phys. Lett. B **666**, 228 (2008); C. B. Chiu and R. C. Hwa, Phys. Rev. C **79**, 034901 (2009).

[6] C. Tsallis, J. Stat. Phys. **52**, 479 (1988); Eur. Phys. J. A **40**, 257 (2009); cf. also *Introduction to Nonextensive Statistical Mechanics* (Springer, Berlin, 2009). For an updated bibliography on this subject, see http://tsallis.cat.cbpf.br/biblio.htm.

[7] F. S. Navarra, O. V. Utyuzh, G. Wilk, and Z. Włodarczyk, Phys. Rev. D **67**, 114002 (2003); M. Rybczyński, Z. Włodarczyk, and G. Wilk, Nucl. Phys. B, Proc. Suppl. **122**, 325 (2003); G. Wilk and Z. Włodarczyk, J. Phys. G **38**, 065101 (2011).

[8] G. Wilk and Z. Włodarczyk, Eur. Phys. J. A **48**, 161 (2012).

[9] G. Wilk and Z. Włodarczyk, Central Eur. J. Phys. **10**, 568 (2012); G. Wilk and Z. Włodarczyk, Eur. Phys. J. A **40**, 299 (2009); M. Rybczyński, Z. Włodarczyk, and G. Wilk, J. Phys. G **39**, 095004 (2012).

[10] T. Wibig, J. Phys. G **37**, 115009 (2010).

[11] K. Ürmössy, G. G. Barnaföldi, and T. S. Biró, Phys. Lett. B **701**, 111 (2011); **718**, 125 (2012).

[12] J. Cleymans and D. Worku, J. Phys. G **39**, 025006 (2012); J. Cleymans and D. Worku, Eur. Phys. J. A **48**, 160 (2012).

[13] T. S. Biró, K. Ürmössy, and Z. Schram, J. Phys. G **37**, 094027 (2010); T. S. Biró and P. Ván, Phys. Rev. E **83**, 061147 (2011); T. S. Biró and Z. Schram, Eur. Phys. J. Web Conf. **13**, 05004 (2011); T. S. Biró, *Is there a Temperature? Conceptual Challenges at High Energy, Acceleration and Complexity* (Springer, New York Dordrecht Heidelberg London, 2011).

[14] B. Andersson, G. Gustafson, and T. Sjöstrand, Z. Phys. C **20**, 317 (1983); B. Andersson, G. Gustafson, G. Ingelman, and T. Sjöstrand, Phys. Rep. **97**, 31 (1983); T. Sjöstrand and M. Bengtsson, Comput. Phys. Commun. **43**, 367 (1987); B. Andersson, G. Gustavson, and B. Nilsson-Alqvist, Nucl. Phys. **B281**, 289 (1987).

[15] R. Blankenbecler and S. J. Brodsky, Phys. Rev. D **10**, 2973 (1974).

[16] R. Blankenbecler, S. J. Brodsky, and J. Gunion, Phys. Rev. D **12**, 3469 (1975).

[17] E. A. Schmidt and R. Blankenbecler, Phys. Rev. D **15**, 3321 (1977).

[18] R. Blankenbecler, Report No. SLAC-PUB-2077, 1977.

[19] C. Y. Wong, *Introduction to High-Energy Heavy-Ion Collisions* (World Scientific, Singapore, 1994).

[20] T. Sjöstrand and M. van Zijl, Phys. Rev. D **36**, 2019 (1987); R. Corke and T. Sjöstrand, J. High Energy Phys. 03 (2011) 032; T. Sjöstrand and P. Z. Skands, Eur. Phys. J. C **39**, 129 (2005); J. High Energy Phys. 03 (2004) 053; R. Corke and T. Sjöstrand, J. High Energy Phys. 01 (2010) 035.

[21] F. Arleo, S. Brodsky, D. S. Hwang, and A. M. Sickles, Phys. Rev. Lett. **105**, 062002 (2010).

[22] S. Brodsky, G. de Teramond, and M. Karliner, Annu. Rev. Nucl. Part. Sci. **62**, 1 (2012).

[23] J. Adams *et al.* (STAR Collaboration), Phys. Rev. D **74**, 032006 (2006).

[24] T. A. Trainor, Phys. Rev. C **78**, 064908 (2008); T. A. Trainor and D. T. Kettler, Phys. Rev. D **74**, 034012 (2006); T. A. Trainor, Phys. Rev. C **80**, 044901 (2009); J. Phys. G **37**, 085004 (2010).

[25] B. I. Abelev *et al.* (STAR Collaboration), Phys. Rev. C **75**, 064901 (2007).

[26] A. Adare *et al.* (PHENIX Collaboration), Phys. Rev. D **83**, 052004 (2011).

[27] V. Khachatryan *et al.* (CMS Collaboration) J. High Energy Phys. 02 (2010) 041; Phys. Rev. Lett. **105**, 022002 (2010).

[28] S. Chatrchyan *et al.* (CMS Collaboration) J. High Energy Phys. 08 (2011) 086.

[29] G. Aad *et al.* (ATLAS Collaboration), New J. Phys. **13**, 053033 (2011).

[30] K. Aamodt *et al.* (ALICE Collaboration), Phys. Lett. B **693**, 53 (2010); Eur. Phys. J. C **71**, 1594 (2011); **71**, 1655 (2011).

[31] C. Michael and L. Vanryckeghem, J. Phys. G **3**, L151 (1977); C. Michael, Prog. Part. Nucl. Phys. **2**, 1 (1979).

[32] G. Arnison *et al.* (UA1 Collaboration), Phys. Lett. **118B**, 167 (1982).

[33] C. Y. Wong and G. Wilk, Acta Phys. Pol. B **43**, 2047 (2012).

[34] G. Wilk and Z. Włodarczyk, Acta Phys. Pol. B **35**, 871 (2004); **35**, 2141 (2004).

[35] M. Rybczyński, Z. Włodarczyk, and G. Wilk, Nucl. Phys. B, Proc. Suppl. **97**, 81 (2001).

[36] S. J. Brodsky and G. Farrar, Phys. Rev. Lett. **31**, 1153 (1973); Phys. Rev. D **11**, 1309 (1975).

[37] V. Matveev, R. Muradyan, and A. Tavhelidze, Nuovo Cim. Lett. **7**, 719 (1973).

[38] C. White *et al.*, Phys. Rev. D **49**, 58 (1994).

[39] K. Kastella, Phys. Rev. D **36**, 2734 (1987).

[40] G. Calucci and D. Treleani, Phys. Rev. D **41**, 3367 (1990).

[41] G. Calucci and D. Treleani, Phys. Rev. D **44**, 2746 (1991).

[42] G. Calucci and D. Treleani, Int. J. Mod. Phys. A **06**, 4375 (1991).

[43] G. Calucci and D. Treleani, Phys. Rev. D **49**, 138 (1994).

[44] G. Calucci and D. Treleani, Phys. Rev. D **50**, 4703 (1994).

[45] G. Calucci and D. Treleani, Phys. Rev. D **63**, 116002 (2001).

[46] A. Accardi and D. Treleani, Phys. Rev. D **64**, 116004 (2001).

[47] M. Gyulassy, P. Levai, and I. Vitev, Nucl. Phys. **B594**, 371 (2001).

[48] R. Corke and T. Sjöstrand, J. High Energy Phys. 01 (2010) 035.

[49] F. Abe *et al.* (CDF Collaboration), Phys. Rev. Lett. **70**, 1376 (1993).

[50] B. Abbott *et al.* (D0 Collaboration), Phys. Rev. D **64**, 032003 (2001).

[51] D. E. Acosta *et al.* (CDF Collaboration), Phys. Rev. D **65**, 112003 (2002).

[52] B. Abbott *et al.* (D0 Collaboration), Phys. Rev. Lett. **84**, 2786 (2000).

[53] V. M. Abazov *et al.* (D0 Collaboration), Phys. Rev. Lett. **87**, 251805 (2001).

[54] C. Y. Wong and H. Wang, Phys. Rev. C **58**, 376 (1998).

[55] R. Gastman and T. T. Wu, *The Ubiquitous Photon* (Clarendon Press, Oxford, 1990).

[56] R. Blankenbecler, A. Capella, C. Pajares, J. Tran Thanh Van, and A. Ramallo, Phys. Lett. **107B**, 106 (1981); C. Pajares and A. V. Ramallo, Phys. Rev. D **31**, 2800 (1985); D. Treleani, Int. J. Mod. Phys. A **11**, 613 (1996).

[57] Beringer *et al.* (Particle Data Group), Phys. Rev. D **86**, 010001 (2012).

[58] D. W. Duke and J. F. Owens, Phys. Rev. D **30**, 49 (1984).

[59] S. Chekanov *et al.* (ZEUS Collaboration), Phys. Rev. D **67**, 012007 (2003).

[60] S. Chekanov *et al.* (ZEUS Collaboration), Eur. Phys. J. C **42**, 1 (2005).

[61] B. Abelev *et al.* (ALICE Collaboration), Phys. Lett. B **722**, 262 (2013).

[62] J. Binnewies, B. A. Kniehl, and G. Kramer, Z. Phys. C **65**, 471 (1995).

[63] M. Bengtsson and T. Sjöstrand, Nucl. Phys. **B289**, 810 (1987); E. Norrbin and T. Sjöstrand, Nucl. Phys. **B603**, 297 (2001).

[64] G. Marchesini and B. R. Webber, Nucl. Phys. **B238**, 1 (1984); G. Corcella, I. G. Knowles, G. Marchesini, S. Moretti, K. Odagiri, P. Richardson, M. H. Seymour, and B. R. Webber, J. High Energy Phys. 01 (2001) 010.

[65] G. Gustafson, Phys. Lett. B **175**, 453 (1986); G. Gustafson and U. Pettersson, Nucl. Phys. B **306**, 746 (1988); L. Lönnblad, Comput. Phys. Commun. **71**, 15 (1992).

[66] C. Y. Wong and R. Blankenbecler, Phys. Rev. C **22**, 2433 (1980).

[67] S. Chatrchyan *et al.* (CMS Collaboration), Phys. Rev. Lett. **107**, 132001 (2011); arXiv:1212.6660 [Phys. Rev. D (to be published)].